Master Thesis

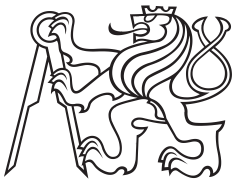

Czech Technical University in Prague

F3

Faculty of Electrical Engineering
Department of Electromagnetic field

Increase of the Sensitivity of Object Detection by the LiDAR Systems

Bc. Vojtěch Krča

Supervisor: prof. Ing. Stanislav Zvánovec, Ph.D.
Supervisor–specialist: Ing. Tomáš Němeček, Ph.D.
Field of study: Electronics and Communications
Subfield: Photonics
May 2022

ZADÁNÍ DIPLOMOVÉ PRÁCE

I. OSOBNÍ A STUDIJNÍ ÚDAJE

Příjmení: **Krča** Jméno: **Vojtěch** Osobní číslo: **465886**

Fakulta/ústav: **Fakulta elektrotechnická**

Zadávající katedra/ústav: **Katedra elektromagnetického pole**

Studijní program: **Elektronika a komunikace**

Specializace: **Fotonika**

II. ÚDAJE K DIPLOMOVÉ PRÁCI

Název diplomové práce:

Zvýšení citlivosti detekce objektů u LIDARových systémů

Název diplomové práce anglicky:

Increase of the Sensitivity of Object Detection by the LIDAR Systems

Pokyny pro vypracování:

Cílem diplomové práce je teoretická rešerše, rozbor, návrh možných zapojení a následná realizace experimentální konfigurace detekce vzdálených objektů LIDARovým systémem.
Student se prvotně zaměří na teoretický rozbor možných konfigurací měření vzdálenosti objektů laserovým paprskem, zároveň zváží dostupnost komponent na jejich pozdější realizaci. V práci rozebere pokročilejší metody, které jsou schopny zlepšit rozlišení detekce, jako jsou například heterodynní detekce, využití lock-in zesilovače či frekvenčně modulované kontinuální lasery (FMCW LIDAR). Z uvedených zapojení se zaměří především na potřebný zdroj a detekční metodu/jednotku.
Základem praktické části pak bude návrh zapojení a experimentálního uspořádání zvolené metody. Po postavení a optimalizaci tohoto zapojení naměřte jeho charekteristiky pro různé cíle. Hlavní zaměření bude kladeno na vysílací a přijímací část s cílem zlepšit limit detekce klasické TOF (Time-of-Flight) metody.

Seznam doporučené literatury:

[1] P. F. McManamon, LiDAR Technologies and Systems, SPIE, 2019.
[2] S. Muckenhuber, H. Holzer, Z. Bockaj, Automotive Lidar Modelling Approach Based on Material Properties and Lidar Capabilities. Sensors 2020, 20, 3309.
[3] C. Kim, Y. Jung, S. Lee, FMCW LiDAR System to Reduce Hardware Complexity and Post-Processing Techniques to Improve Distance Resolution. Sensors 2020, 20, 6676.

Jméno a pracoviště vedoucí(ho) diplomové práce:

prof. Ing. Stanislav Zvánovec, Ph.D. katedra elektromagnetického pole FEL

Jméno a pracoviště druhé(ho) vedoucí(ho) nebo konzultanta(ky) diplomové práce:

Ing. Tomáš Němeček VALEO

Datum zadání diplomové práce: **07.09.2021** Termín odevzdání diplomové práce: **20.05.2022**

Platnost zadání diplomové práce: **19.02.2023**

prof. Ing. Stanislav Zvánovec, Ph.D. podpis vedoucí(ho) práce	podpis vedoucí(ho) ústavu/katedry	prof. Mgr. Petr Páta, Ph.D. podpis děkana(ky)

III. PŘEVZETÍ ZADÁNÍ

Diplomant bere na vědomí, že je povinen vypracovat diplomovou práci samostatně, bez cizí pomoci, s výjimkou poskytnutých konzultací.
Seznam použité literatury, jiných pramenů a jmen konzultantů je třeba uvést v diplomové práci.

. _____
Datum převzetí zadání

_____
Podpis studenta

Acknowledgements

I would like to thank everyone who participated on this thesis for their help and support. Special thanks goes to Tomáš Němeček for providing know-how and for his precious time. I thank my family and friends, namely the so-called FELita group, for support and stress relieve. Finally I would like to acknowledge FEE CTU for the provided education.

Declaration

I declare I have accomplished my bachelor project by myself and I have named all the sources used in accordance with the Guideline on ethical preparation of university theses.

In Prague, 19. May 2022

Abstract

This thesis describes LiDARs, their components, features and applications. Thesis focuses on increasing of the sensitivity of LiDARs. Different methods for distance measurement and object detection with LiDAR are proposed. Methods of pulsed time of flight and amplitude modulated continuous wave LiDAR are evaluated by measurements with a test setup that is designed, built and modified for more precise results. This thesis further presents comparison of those methods via processing of measured signals. All findings obtained from theoretical and practical parts of this thesis are summarised in the conclusion.

Keywords: LiDAR, ranging, detection sensitivity

Supervisor: prof. Ing. Stanislav Zvánovec, Ph.D.
Katedra elektromagnetického pole
Technická 2, B2-533
Praha

Abstrakt

Tato práce popisuje LiDARy, jejich komponenty, vlastnosti a aplikace. Práce se zaměřuje na zvýšení citlivosti LiDARů. Jsou navrženy odlišené metody pro měření vzdálenosti a detekci objektů LiDARem. Metody pulzní doby letu (time of flight) a amplitudově modulovaného kontinuálního LiDARu jsou ověřeny měřením na testovacím přípravku, který je v rámci této práce navržen, sestaven a následně modifikován pro přesnější výsledky. Práce dále prezentuje porovnání těchto metod díky zpracování naměřených signálů. Všechny poznatky nabité z teoretické i praktické části jsou shrnuty v závěru práce.

Klíčová slova: LiDAR, měření vzdálenosti, citlivost detekce

Překlad názvu: Zvýšení citlivosti detekce objektů u LiDARových systémů

Contents

Acronyms 1

1 Introduction to LiDAR systems 3

1.1 What is LiDAR 3

1.2 Phenomena affecting LiDAR design and its performance 4

1.2.1 Wavelength 4

1.2.2 Atmospheric effects 5

1.2.3 Eye safety 6

1.2.4 Other parameters 8

1.3 Sources and detectors 9

1.3.1 Laser sources for LiDAR 9

1.3.2 Detectors for LiDAR 10

1.4 Applications of LiDAR 11

2 Theory for advanced LiDAR systems and detection methods 13

2.1 Time of flight LiDAR 15

2.1.1 Calculation of general parameters for ToF LiDAR 16

2.2 Amplitude modulated LiDAR . . 17

2.3 Coherent LiDAR (with heterodyne detection) 18

2.3.1 Frequency modulated continuous wave LiDAR 20

2.3.2 Lock-in amplifier 21

3 Experimental part 23

3.1 The optical fibre setup 23

3.1.1 Design 23

3.1.2 Components 24

3.1.3 Measurements 25

3.2 The free space setup 29

3.2.1 Design 29

3.2.2 Components 30

3.2.3 Preparation of the setup and alignment 31

3.2.4 Measurements 32

3.2.5 Data processing 36

3.3 The improved free space setup . . 37

3.3.1 Design 37

3.3.2 Components 37

3.3.3 Measurements 38

4 Conclusion **43**

Bibliography **45**

A Figures **49**

Acronyms

AELs Accessible emission limits.

AM Amplitude Modulator.

AMCW Amplitude Modulated Continuous Wave.

APD Avalanche Photodiode.

BS beamsplitter.

BW bandwidth.

CCD charge-coupled device.

CMOS complementary metal-oxide semiconductor.

EO electro-optical.

FIR far infra-red.

FMCW Frequency Modulated Continuous Wave.

FoV field of view.

FWHM Full width at half maximum.

IEC International Electrotechnical Commission.

IR infra-red.

LADAR LAser Detection And Ranging.

LD laser diode.

LED light-emitting diode.

LiDAR Light Detection And Ranging.

LO local oscillator.

LWIR long-wavelength infra-red.

MEMS Micro-electro-mechanical systems.

MIR mid infra-red.

MPE Maximum permissible exposure.

NIR near infra-red.

PD Photodiode.

RF radio frequency.

SNR signal-to-noise ratio.

ToF Time of Flight.

VCSEL vertical-cavity surface-emitting laser.

Chapter 1

Introduction to LiDAR systems

1.1 What is LiDAR

LiDAR stands for Light Detection And Ranging. LiDAR as it's name suggests is used for object detection and distance measurements based on captured time delay. Terms that are also used include LIDAR, LADAR, laser scanner or laser radar and they can be used interchangeably despite having different historical background [1]. The word LiDAR with this specific capitalisation is used in academic literature that I cite here but also in commercial applications. The term LiDAR is used throughout this thesis as a reference to the technology itself and for the whole system as well. This thesis mainly focuses on the components, signal transmission and detection and also signal processing.

LiDAR's basic principle is that it transmits a light beam which is reflected from a target and it is received on the detector. That makes it an active device as opposed to passive electro-optical (EO) sensors which rely on ambient light only[1]. For example cameras detect ambient light reflected from objects as opposed to LiDARs for which ambient light is considered as noise. LiDAR usually consists of electrical, optical and mechanical components. It is composed mainly of a laser source as a transmitter, detector or array of detectors as a receiver, an optical system (usually lenses and mirrors) for focusing and directing the light beam, an optical band pass filter and electronics for data transfer and evaluation. This is accompanied by mechanical components to hold components together with proper alignment and housing

[1] Specialised sensors could also rely on blackbody radiation of objects.

for protection. For measurement itself also environment (attenuation, noise, multi-path reflections) and target characteristic (reflection, attenuation) need to be taken into consideration [2].

LiDARs are a well understood technology as the technology was firstly described and used more than 50 years ago [3]. A lot of research was done and they have been developed into many forms with different applications. LiDARs serve different distance measuring and 3D scanning purposes ranging from terrain monitoring through civil engineering, to automotive purposes. The vast list of use cases for LiDAR is continued in Section 1.4. When LiDARs' parameters are tweaked they can be designed for different visibility scenarios (E.g. cloudy or foggy conditions) or for different distances ranging from centimetres to kilometres.

1.2 Phenomena affecting LiDAR design and its performance

In the following paragraphs, different aspects for developing a LiDAR system are described.

1.2.1 Wavelength

LiDARs usually operate at around 1 or 1,5μm wavelength which corresponds to 300 THz or 200 THz, respectively via

$$c = \lambda f, \tag{1.1}$$

where $c = 3 \cdot 10^8$ ms^{-1} is the speed of light, λ is wavelength and f is frequency. This is referred to as near infra-red (NIR) part of the electromagnetic spectrum. Those frequencies are used because of a low attenuation through atmosphere, for eye safety reasons and because of common laser technologies for these wavelengths. Wavelength of 1550 nm is a good choice as it is already widely adopted in communications industry and there is a good transmission through OH^- particles. Aspects for choosing a fitting frequency are discussed in the following subsections. But different frequencies from the visible and infra-red (IR) regions of the spectrum are also used for specific applications that are described later.

LiDARs share similarities with radars which work in a different frequency

range (microwave). That allows radars to detect better through fog and clouds but allows worse angular resolution and a sufficient detection only for metal objects. See Fig. 1.1 for information in which part of the electromagnetic spectrum LiDAR and radar operate and for comparison with other technologies.

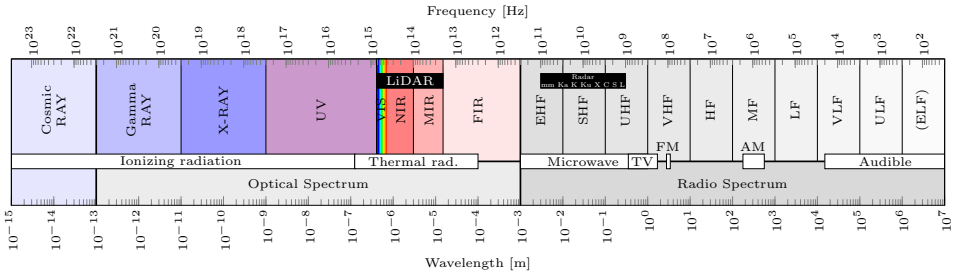

Figure 1.1: Electromagnetic spectrum with dual logarithmic axis. Displayed to show in which parts of the spectrum LiDAR and radar operate [4]. Inspired by [5].

1.2.2 Atmospheric effects

As previously mentioned, atmospheric effects are causing attenuation and scattering of light on its way from point A to B and therefore giving physical limits to the LiDAR technology. Therefore those effects need to be taken into consideration when designing a LiDAR system. Atmospheric effects are also one of the reasons for choosing a specific wavelength for LiDAR. There are two most noticeable effects, atmospheric absorption and atmospheric scattering, that are described in the following paragraphs.

Atmospheric absorption is caused mainly by water molecules and is therefore noticeable mainly in places with higher humidity and especially in summer. It mostly affects light in the long-wavelength infra-red (LWIR) spectral range (8-14 μm, between MIR and FIR on Fig. 1.1). Absorption transforms electromagnetic energy of the light into internal energy of the molecule (mainly in form of heat) [2]. Atmospheric absorption and its major components in relation to wavelength can be seen in Fig. 1.2.

Another attenuation to the propagation of light through atmosphere is added by scattering. Light is deviated from its original path. Rayleigh scattering on particles with size much smaller (with diameter d) than signal wavelength (λ) is inverse proportional to wavelength ($I \sim \frac{d^6}{\lambda^4}$). Mie scattering scatters light mainly into the forward direction and happens on particles with size similar to wavelength. The scattering effect is not only attenuat-

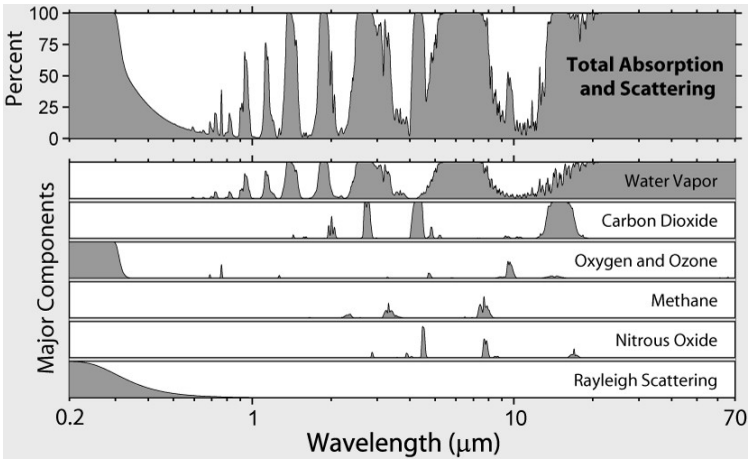

Figure 1.2: Absorption by the atmosphere for wavelengths in visible and IR parts of the spectrum and its major components. Adapted from [6].

ing the signal but can be utilised for some special applications such as in multiwavelenght LiDARs for atmospheric and ocean sensing [2].

1.2.3 Eye safety

A very important aspect of LiDAR development is eye safety or laser safety. Eye retina or surface of the eye could be damaged by laser radiation and therefore precautions need to be taken. Standards like IEC 60825 [7] provide detailed classification of laser products and regulations to protect human eyes. Accessible emission limits (AELs) are defined at certain wavelengths for both average energy and peak power for each Class. Laser sources are divided into classes based on their ability to damage human tissue. Those classes are categorised by two parameters: maximum output power and wavelength (see Fig. 1.3). Laser classes (according to [8]) are:

- **Class 1**: Safe unless optics for magnification is used.
- **Class 2**: Safe because of blink reflex. (400-700 nm, $\leq$ 1 mW continuous-wave, see further paragraphs)
- **Class 3R**: Safe if handled properly.
- **Class 3B**: Hazardous with direct eye exposure, might need goggles.
- **Class 4**: Lasers can burn the skin and damage the eye.

In the IEC 60825 norm there are also requirements that every manufacturer needs to supply demanded information and provide warning labels and instructions.

Figure 1.3: Maximal allowed continuous power for different wavelengths defined for different laser classes based on EN 60825 norm. From [9] (Created under Creative Commons license).

Based on experiments Maximum permissible exposure (MPE) of light on the human eye was established and is shown in Fig. 1.4. MPE is a highest possible energy density that is safe for the human eye [8]. MPE is dependant on wavelength but also on pulse width or pulse duration in case of pulsed source or on exposure time. Scanning LiDAR has an advantage of lower average exposure and it can therefore emit higher power beam because it utilises pulsed laser. This is a limiting factor for a continuous wave LiDAR.

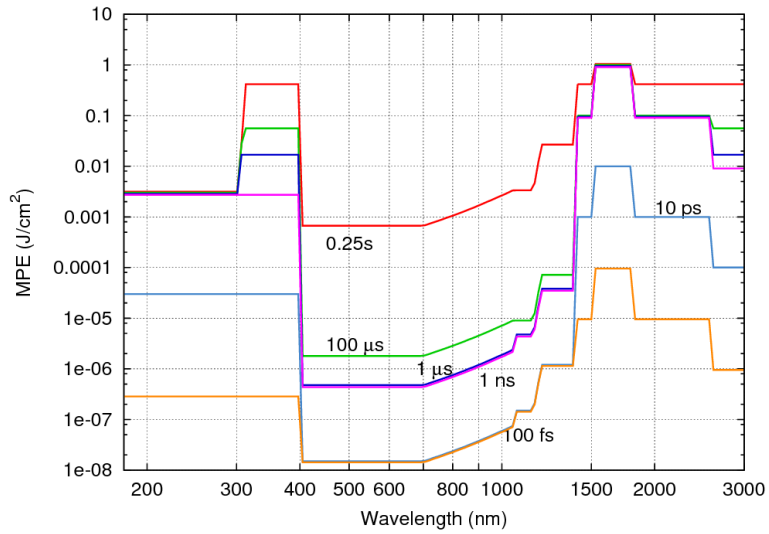

Figure 1.4: Maximum permissible exposure (MPE) given in energy density (energy per area of the aperture, J/cm^2), for different exposure times and various wavelengths. Source [10], based on IEC 60825 formulas.

Safe laser power levels are determined based on a response of the human eye. Water present in the human eye partially blocks transmission of light with wavelengths below 0.4 μm and above 1.5 μm. Also the blinking effect provides a certain layer of safety for lasers with wavelength in the visible part of the electromagnetic spectrum. The human eye blinks when an exceedingly bright light approaches it thus saving it from permanent exposure to high power laser light that would otherwise damage it. Laser class 2 is based on this knowledge.

1.2.4 Other parameters

There are three important parameters to be considered for LiDAR development that affect the properties of the LiDAR systems. Those parameters are measurement method (mostly for distance measurement), wavelength (by which the transmission and reception technology is chosen as briefly mentioned) and scanning technology (pointing beam into directions) [8]. Wavelength was already described in detail, measurement methods are shown here and extended on in Chapter 2 and scanning technology is also briefly mentioned throughout this thesis. Other parameters are reported in the following paragraphs.

Distance measurement techniques based on different modulation and demodulation schemes are direct Time of Flight (ToF) LiDAR with pulsed laser source, Amplitude Modulated Continuous Wave (AMCW) that also calculates a time of flight but from a continuous signal and Frequency Modulated Continuous Wave (FMCW) which captures a phase difference [11]. Some LiDAR systems also use other specific methods and different types of modulations (E.g. pseudo random code waveform) as presented in [2, 12].

Noise is a major parameter and LiDAR systems should try to eliminate as much noise as possible to improve their signal-to-noise ratio (SNR). Noise is usually introduced as a background noise. Light sources such as street lamps or car headlamps, radiation from the sun or laser sources in different LiDAR systems are considered as background noise. Background noise can be reduced by using band pass filters [8]. Other forms of noise like dark current or thermal noise are added on the detector. Amplifying the signal could also introduce additional noise.

Parameters mentioned in this section are affecting the decision of which of the LiDAR type to develop. LiDAR imaging (measuring range in multiple angular positions, also called 3D LiDAR) could be utilised in those ways

based on distance measurement techniques and with parameters that are described in Chapter 2.

1.3 Sources and detectors

As already mentioned in this thesis, sources and detectors are important components for LiDARs. Transmitting modulated light for ranging purposes requires fast, coherent and low divergent sources with narrow spectral linewidth. Therefore the best source for this purpose is laser.

1.3.1 Laser sources for LiDAR

Laser in general consists of a resonator that is composed of one mirror and a second mirror which is semitransparent, switchable or with a small hole. They further consist of a medium and a pump. Laser sources can be divided into certain categories based on the material of their medium (gases, liquids or solids). Materials for solid state laser's medium include insulating solids (crystals, ceramics or glasses) and added dopants. Two dominant categories of solid state laser exist: bulk and fibre [13]. Lasers exist in different form factors. Laser diodes and fibre lasers are popular for modern LiDARs while gassed lasers are not used any more. Fibre lasers offer good efficiency and are easy for connection and alignment. They are also great for high repetition rate or continuous regimes but they are limited for peak power because of their small cross section [8].

Diode lasers are the cheapest and the most efficient with wall plug efficiency of more than 30% according to [8]. They only need a current passing through their P-N junction to excite the laser. Therefore diode lasers are great not only for short range standalone applications but also for pumping other forms of lasers for higher power. Q-switched lasers need to be used to accumulate enough energy into a nanosecond-class pulse. Laser diodes are not capable of longer ranges than hundreds of meters as there is not enough energy in their longer pulses.

There are many technologies that could be used according to designated wavelength. Lasers are manufactured with different technologies thus producing different wavelengths (E.g. CO_2 laser @10.6 μm, Nd:YAG @1064 nm or AlGaAs @850 nm). Mostly visible or infra-red (IR) wavelengths are used

out of which near infra-red (NIR) is the most common for use in LiDAR. Especially popular are Si lasers and receivers because of their price, but their maximal wavelength is around 1.1 μm due to their band gap of 1.12 eV. Silicon based laser diode (LD) or vertical-cavity surface-emitting laser (VCSEL) is used for cost reasons. They usually have a wavelength of 905 nm.

1.3.2 Detectors for LiDAR

Detector needs to be fast and low noise which suggests using a Photodiode (PD). Ideally a detector with high gain for low power, low reflectivity or long distance scenarios is needed and therefore avalanche Avalanche Photodiode (APD) is often used. Higher gain (state of the art goes up to 1000) is achieved because one photon can generate multiple electrons in the APD. High gain is needed as there is a demand for high range LiDAR but also sources can not exceed eye safe power limits and targets are often not very reflective (most LiDARs deal with Lambertian surfaces). Therefore correct bias circuit is needed for the APD and also amplification electronics can be applied to the radio frequency (RF) signal. Other option to increase gain is to use fiber pre-amplifier [8].

On the other hand coherent LiDAR which is described thoroughly in Chapter 2 does not require gain and sensitivity is increased thanks to the coherent detection itself [8]. Therefore normal photo-detectors can be used.

For some applications arrays of detectors are deployed when the resolution needs to be increased. Multiple PDs or APDs can be put into a 1D array. Another option is to use 2D sensors made with a complementary metal-oxide semiconductor (CMOS) technology which is low power and easier to integrate with other electronics. Second technology for 2D sensors is charge-coupled device (CCD) with potential for a better signal to noise ratio (SNR) but CCD is slower than CMOS and over-saturation can cause blooming[2] [14]. Article [15] recommends using electron-multiplying CCD with a typical gain of 100x. Secondly, field guide [8] suggests using gated 2D imaging. This method proposes to only open the shutter in small time period when the laser pulse should return. This could reduce noise.

One of the issues of LiDAR's detectors is blooming. The detectors need to be very sensitive to detect reflections from Lambertian surfaces of great

[2]LiDAR blooming is also mentioned in this section but it should not be confused with CCD's blooming effect during which charge that should be present only in one pixel is spilled to neighbouring ones.

distance. Therefore reflection from highly reflective surfaces with mirror-like finishes or retroreflectors reflect too much power. This results in LiDAR seeing the object bigger and closer or further than it is in reality. Software algorithms need to be applied to mitigate this effect.

1.4 Applications of LiDAR

LiDARs sense either the geometry, the surface or movements of objects and many parameters can be captured (or calculated) including reflectivity, spectral parameters, polarization, Doppler shift and 3D data (point cloud) which offers broad variety of use-cases. LiDARs were primarily developed for military operations (rangefinders, designators, target detection, weapon guidance, tracking, obstacle avoidance systems, velocimetry and vibrometry) but proved themselves useful in the fields of medicine (OCT, abberometry and orthopaedic modeling), manufacturing (object detection), astrology (long distance range measurements and altimeters for Moon surface), agriculture (land field or forest mapping and remote sensing of vegetation), cartography (3D mapping) and meteorology (wind sensing) [2, 16, 3, 17]. As LiDARs get cheaper and widely available they find use cases in consumer electronics (robotic vacuum cleaners or mobile phone cameras), marketing and commerce (E.g. monitoring people flow in supermarkets which could also be used for security) and in interactive entertainment and gaming (3D motion detection for gaming consoles, 3D scanning for virtual reality and other human-computer interactions). Another big market is predicted to be robots in industrial applications (construction and factory automation) [2, 17, 18]. This exhaustive list of applications demonstrates how versatile LiDARs are. Fig. 1.5 shows some of those applications in picture and it also suggests certain technologies that could be used in LiDAR systems.

The biggest demand now is in the automotive industry especially for Advanced driver-assistance systems (ADAS) or fully autonomous vehicles in the future. LiDARs are useful for SAE J3016 [19] Automation Levels from 2 to 5. As of 2022, cars with level 3 are already in production [20], meaning they can take full control over the car without driver's attention in certain scenarios. Bigger redundancy is needed for higher levels of automation and therefore data from multiple sensors are used (LiDAR in cooperation with camera and radar). This is referred to as sensor fusion. As opposed to cameras, using LiDARs for range measurement in automotive sector provides better performance in darkness or direct sunlight thanks to active measurement and they also provide range information directly. Cameras also have an issue of interference from light beams from other cars. LiDAR exceeds radar with fine granularity of information, better detection in rain and good object detection

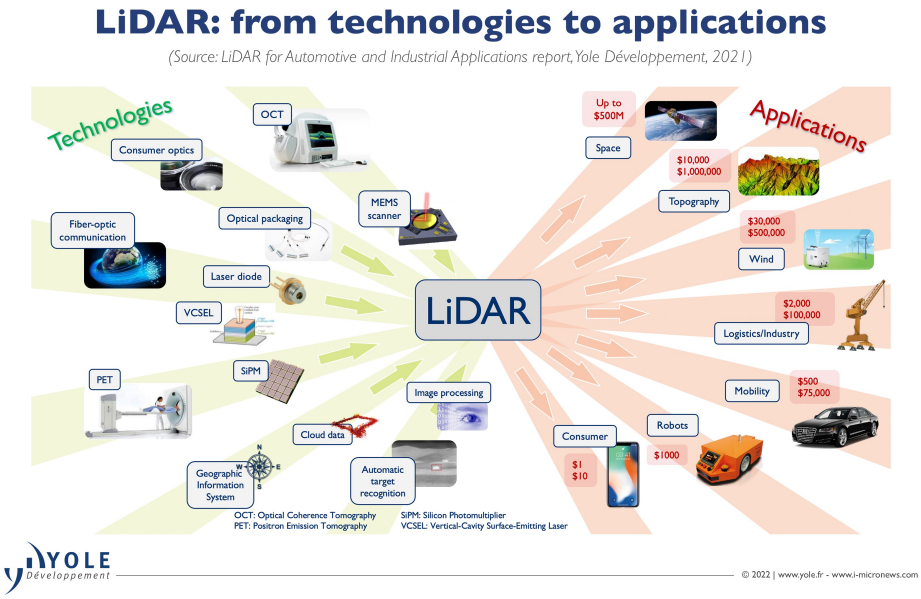

Figure 1.5: Examples of technologies and applications according to LiDAR market report. Prices of the LiDAR itself and of the whole product are displayed. Obtained from Yole Development [18] with permission to use.

thanks to good resolution. Radars also suffer from higher noise.

The most common version of LiDAR for range measurements and object detection is time of flight LiDAR (ToF) which transmits short pulses and measures time until they reach the detector. This is the easiest and most robust approach. It is described in the following Chapter 2 together with some different and more advanced methods for enhancing LiDAR sensitivity. Also techniques for measuring other parameters than range are described. One of these methods is than chosen and experimentally evaluated in the following chapters. In Chapter 3 all laboratory setups are designed, described, tested and measurement results are presented. Everything is then summarised in Chapter 4.

Chapter 2

Theory for advanced LiDAR systems and detection methods

Specific methods for LiDAR object detection, ranging, velocimetry and for other applications are introduced in this chapter. Firstly time of flight method is shown, then amplitude modulation for LiDAR is described and finally coherent LiDAR with focus on frequency modulation is presented. Comparison of these methods and their functioning principles are shown in Fig. 2.1.

The biggest difference between these methods is the demand on the laser source and detector. ToF method needs a laser with high power in a short pulse while other mentioned methods utilise sources for continuous power. FMCW needs the most advanced source as the wavelength needs to be modulated. Receivers and signal processing are also very different and they need to be adapted to the used method. ToF detector needs to be fast, AMCW can have lower bandwidth (BW) as the sine wave can be reconstructed from fewer samples than a single pulse. FMCW detector is the most complex, it needs to combine local oscillator (LO) and received signals and do signal processing to demodulate the signal and obtain the beat frequency.

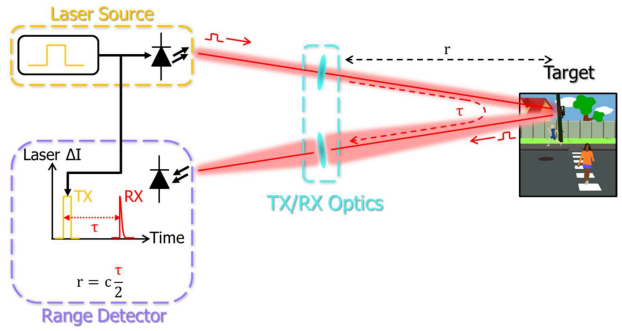

(a) : Pulsed time of flight LiDAR (ToF).

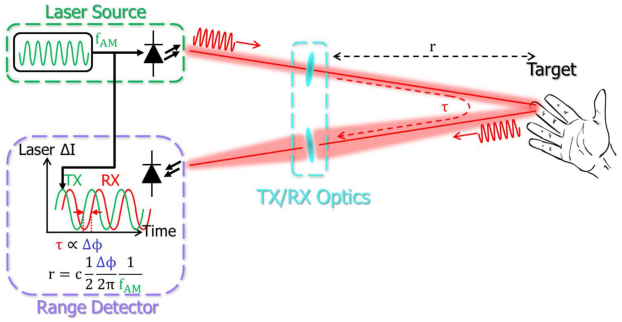

(b) : Amplitude-modulated continuous-wave LiDAR (AMCW).

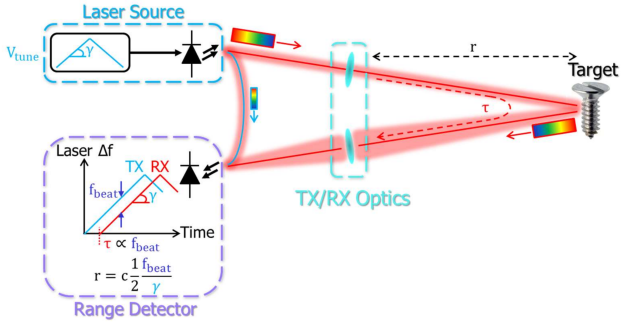

(c) : Frequency-modulated continuous-wave LiDAR (FMCW).

Figure 2.1: Basic schematics and showcases of three different modulation techniques for LiDAR ranging. Adopted from [21].

ToF has an advantage of being easy to implement, components are easily available and cost can be low. AMCW can offer easy and cheap modulation and low demand on detection which makes it good for a flash LiDAR (sometimes called AMCW camera) as a cheap sensor for short range with a wide field of view (FoV). AMCW is already commercialised for indoor applications with CMOS sensors according to [22]. FMCW is able to achieve a very high resolution and can be used for metrology and precision manufacturing but with higher cost and complexity [21]. However FMCW has trouble to sense lateral motion which can be bad for robotic and automotive applications.

And it also can not achieve as long range. Comparison of range and resolution of these architectures can be seen in Fig. 2.2. Detailed explanation of characteristics of these systems follows in next sections.

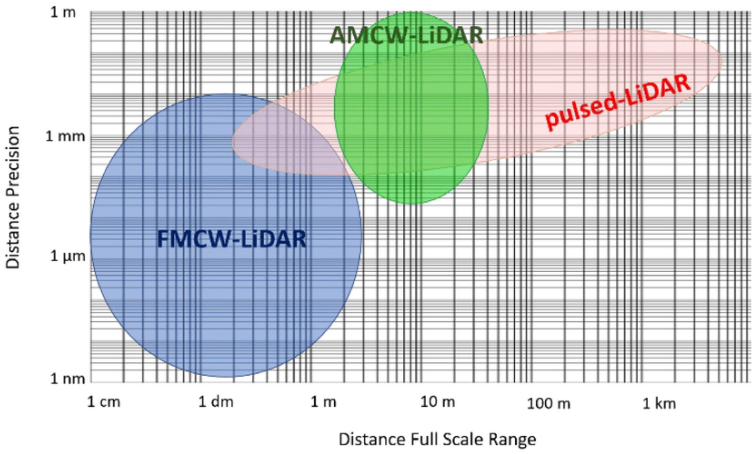

Figure 2.2: Comparison of distance precision and range between ToF, AMCW and FMCW architectures of LiDAR. Copied from [23], original data from [24].

2.1 Time of flight LiDAR

Time of flight LiDAR (ToF) is the mostly used type of LiDAR for range detection systems. The principle is transmitting a short pulse and measuring the time delay between transmission and reception of the pulse on a photodetector. The shape of the illuminator pulse is usually Gaussian or super-Gaussian [8].

ToF method can be applied for scanning LiDAR. To cover a wider screen the collimated beam is swept by a moving mirror. The frequency of the pulse transmission determines the angular resolution while the period of the rotation is a sampling period and therefore time resolution for each point. Alternatively full screen can be illuminated by a laser and an array of detectors can measure ToF. This is called Flash LiDAR. But it brings high demand on detector especially on its sensitivity. Those two types of ToF LiDAR are displayed in Fig. 2.3 and they have the following features:

- Scanner LiDAR:
  - Illuminates and captures the scene point by point based on the position of the scanning mirror.
  - With mechanical rotating elements.

- Cheap (cheap detector: 1 diode or small array to cover the whole elevation angle while scanning only in 1D - horizontally).
- Needs stabilisation.
- Used for: 3D mapping, autonomous driving.
- Two types:
  - LiDAR with rotating mirror that could be also replaced by MEMS micro mirrors.
  - Spinning LiDAR where both transmitter and receiver are rotating as opposed to only rotating the mirror.

- Flash LiDAR:
  - Illuminates and captures the whole environment at once.
    - Usually wide angles are captured.
    - Diffuser is used to spread the light into the FoV.
  - Uses large detector arrays or matrices (CCD or CMOS).
  - Lower demand for stabilisation.
  - Requires a high peak illumination and/or sensitive detectors.

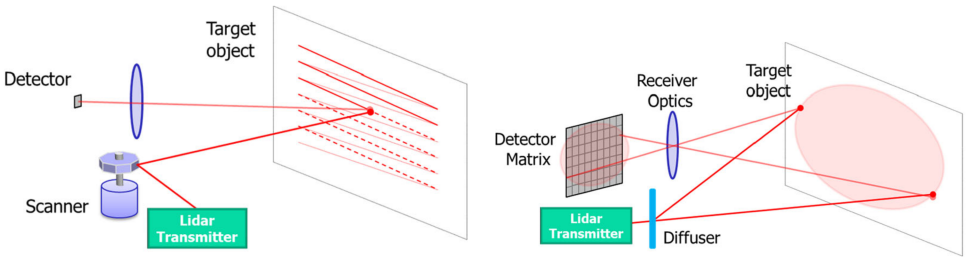

(a) : Scanning LiDAR. **(b) :** Flash LiDAR.

Figure 2.3: Diagrams of scanning and flash LiDARs for comparison. Adopted from [25].

2.1.1 Calculation of general parameters for ToF LiDAR

The object distance (d) is calculated as

$$d = \frac{v\,t}{2}, \tag{2.1}$$

where v is the speed of light in the selected medium (usually air) and t is the actual time of flight. Range resolution of ToF LiDARs is

$$\Delta R = \frac{c}{2\,B}, \tag{2.2}$$

where c is a speed of light for a specific medium and B is a bandwidth of the system ($1/B$ is the pulse width). The rise time of the pulse is also affecting the range [2]. The range resolution can vary from 1 mm to 1 m according to design and application.

Field of view of the LiDAR is

$$FoV = 2 \cdot \arctan\left(\frac{\frac{w}{2}}{f_o}\right), \tag{2.3}$$

where w is a sensor width and f_o is a focal length[1] of the receiving lens. This formula is based on trigonometry and is only valid for angles up to 5° [2]. Typical FoV is lower than 1° for long range applications. In case of automotive industry, vertical FoV is lower (in order of 10°), it needs to be able to recognise small objects on road and decide if a bridge can be passed under. Horizontal FoV is higher (around 100°) to be able to catch vehicles crossing from neighbouring lane with a high detection probability.

Important metric for a scanning ToF LiDAR is its resolution in vertical and horizontal direction. Horizontal resolution is $\frac{i}{360}$, where i is a number of pulses in one rotation. Vertical resolution for systems with more pixels depends on their spacing and position against the lens. Resolution should be at least 1° and even lower for higher range systems.

Full width at half maximum (FWHM) diffraction limit (ϑ) is given by aperture size (D) and wavelength (λ)

$$\vartheta = \frac{1.03\,\lambda}{D}. \tag{2.4}$$

One improvement for ToF LiDAR presented in [2] could be a gated detector that opens only at approximately the time when the beam is expected to arrive. This can eliminate the interference from clutter or scatterings but it also adds complexity.

2.2 Amplitude modulated LiDAR

Another advanced method is Amplitude modulated continuous wave LiDAR (AMCW) which is sometimes called AMCW ToF as it also measures a time

[1] Letter f is used throughout this thesis for frequency therefore f_o is chosen to represent the focal length.

of flight of a light beam. AMCW's principle can be seen in Fig. 2.1b. The biggest difference from a traditional ToF system is that the continuous signal is used instead of a single pulse. The time that it takes for the light to travel from the transmitter to the receiver is derived from the phase difference between transmitted and received signals. Scene is illuminated with intensity modulated signal. Sine wave is usually used. Some systems use other modulations but they have to deal with harmonics as paper [26] suggests.

AMCW LiDARs use continuous-wave laser or light-emitting diode (LED) transmitters. The amplitude can be modulated by varying the bias current into the diode in electrical domain or by external intensity modulators in optical domain [24]. Simplicity and low cost of AMCW systems make them great for shorter range and lower cost indoor applications. But amplitude modulation has also disadvantages like low spatial resolution, low depth precision or limited maximum range [17].

Distance of an object measured with AMCW systems is

$$d = \frac{c}{2} \cdot \frac{\Delta\phi}{2\pi} \cdot \frac{1}{f_{\mathrm{AM}}}, \tag{2.5}$$

where $\Delta\phi$ is a shift in phase between the two sines of frequency f_{AM}. This can be simplified to

$$d = \frac{c\,\Delta t}{2} = \frac{c\,(t_1 - t_2)}{2}, \tag{2.6}$$

where Δt is a time shift between the two phase-shifted sine waves, t_1 and t_2 are time positions of sine peaks if we can calculate their time stamp. Range of a simple AMCW LiDAR can be calculated as

$$R = \frac{c}{2f_{\mathrm{AM}}}. \tag{2.7}$$

2.3 Coherent LiDAR (with heterodyne detection)

Coherent LiDAR mixes a returned optical signal (usually weak) and an optical local oscillator (usually stronger) to capture the phase of the returned signal as illustrated in Fig. 2.1c. The LO needs to be very stable. Mixing occurs on the beamsplitter (beam combiner). This method of extracting signal information in a noisy environment via mixing the detected signal with the local oscillator is called heterodyne detection. The output frequency can be captured on the photodiode (in the electrical domain) and is called beat

frequency. It is usually in orders of Hz to kHz and therefore easy to capture as bandwidth range of photodiodes is higher. The frequency is downshifted by the mixing of signals with similar frequencies, we refer to this as temporal heterodyning. The change in phase of the beat corresponds to the change in phase of the carrier wave.

Coherent LiDAR suffers from the speckle issue due to narrow band of the signal (lasers with linewidth below 1 MHz and therefore with low phase noise are used [11]). Difficulty with exact optical alignment also causes speckle. It can be eliminated with more samples and averaging as it appears randomly. To further increase signal-to-noise ratio (SNR), intensity of the LO should be increased. But with increasing the LO intensity shot noise would become an issue.

Coherent LiDAR is very sensitive as it's electrical level is proportional to the power of an local oscillator unlike traditional ToF LiDAR where electrical level depends on detector sensitivity and gain (which is dependant on the photodiode type, PIN PDs achieve gain of 1 while APDs have gain of 50-100). Coherent LiDAR has gain of up to 10^9 with correct design [27]. It is also more immune to interference as it ignores other frequencies when mixing with the LO. Ambient light or signal from other LiDAR systems is suppressed. PIN photodiode is used for coherent LiDAR because no additional gain is needed and the beat frequency captured on the detector is low frequency.

In heterodyne systems with LO, the output current on the photodetector is

$$I = 2\,E_{\text{sig}}\,E_{\text{LO}}\,\exp[-jt(\omega_{\text{sig}} - \omega_{\text{LO}})], \tag{2.8}$$

where E_{sig} and E_{LO} are electric fields of signal and local oscillator, respectively. ω_{sig} and Variables ω_{LO} are angular frequencies ($\omega = 2\pi f$) of those signals [8]. Balanced heterodyne detection with two photodiodes suppresses LO noise and further increases SNR.

Homodyne detection is a special case of heterodyne detection where signal and LO frequencies are equal (they share a laser source) which enables very precise phase measurements.

Coherent LiDARs enable other applications like velocimetry or remote vibrometry. Doppler effect is used for those applications. It describes the change in frequency (f) with change in velocity (v) according to equation

$$\Delta f = \frac{2v}{\lambda}. \tag{2.9}$$

Remote LiDAR vibrometers can detect the amplitude and frequency of vibrations as speed of the vibration in 1D can be calculated as

$$v = \frac{\mathrm{d}x}{\mathrm{d}t} = \frac{\mathrm{d}}{\mathrm{d}t} A \sin(2\pi f t) = 2\pi f A \cos(2\pi f t). \tag{2.10}$$

Coherent LiDAR is also used in laser speed guns for law enforcement purposes. They allow range and speed measurement in 1D [27].

2.3.1 Frequency modulated continuous wave LiDAR

Frequency modulated continuous wave LiDAR (FMCW) is a special case of a coherent LiDAR. The main difference being a frequency modulation of the transmitted signal. Continuous wave (CW) allows for measuring the velocity via Doppler shift and require the measured object to be moving against the device. An example of a Doppler speed measurement setup is shown in Fig. 2.4. On the other hand, FMCW allows for distance measuring via spectral estimation method [11, 21].

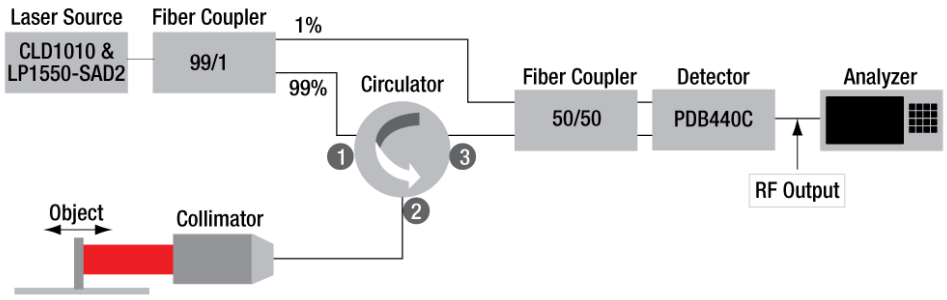

Figure 2.4: Block diagram of a FMCW LiDAR for Doppler speed measurements with Balanced detector for better SNR. Adopted from [28].

Estimated distance to the target is

$$d = \frac{c\,\hat{\tau}}{2} = \frac{c\,\hat{f}_{I_{\mathrm{RX}}}}{2\,\gamma} = \frac{c\,\hat{f}_{I_{\mathrm{RX}}}\,T_{\mathrm{mod}}}{2\,f_{\mathrm{BW}}}, \tag{2.11}$$

where, $\hat{\tau}$ is the time of flight, $\hat{f}_{I_{\mathrm{RX}}}$ is the estimated beat frequency and $\gamma = f_{\mathrm{BW}}/T_{\mathrm{mod}}$ is chirping rate based on f_{BW} which represents modulation bandwidth and modulation period T_{mod}.

An important role in FMCW plays post processing. Fourier transform (usually FFT algorithm) is used to calculate the frequency spectrum and

extract the signal. This is a disadvantage because it cannot happen in real-time.

How to choose modulation frequency based on an achievable range? For RADARs (works for LiDAR too but with change of constant and the SNR of the photodiode is not taken into account):

$$range = \frac{c}{4 \cdot f_{mod}}, \tag{2.12}$$

$$range = 100\text{m} \longrightarrow f_{mod} \leq \frac{c}{4 \cdot r} = \frac{3 \cdot 10^8}{4 \cdot 100} = 750\text{kHz}. \tag{2.13}$$

But it needs to be lower becuase of the BW of the photodetector and speed of the acquisition and FFT calculation. The SNR of the detector and shape of the pulse are also non negligible. On the other hand modulation frequency also needs to be higher than a certain number for real-time object detection (resolution in time).

Coherence length is distance for which a coherent wave maintains it's degree of coherence. For 100 kHz linewidth (laser source CoBrite DX4 as an example) coherence length is

$$\begin{aligned} L &= \sqrt{\frac{2\ln 2}{\pi}} \frac{\lambda^2}{n_{air(@\lambda)} \Delta\lambda} = \sqrt{\frac{2\ln 2}{\pi}} \frac{c}{n_{air(@\lambda)} \Delta f} \\ &= \sqrt{\frac{2\ln 2}{\pi}} \frac{3 \cdot 10^8}{1.0002733 \cdot 100 \cdot 10^3} = 1992.3 \text{ m} \end{aligned} \tag{2.14}$$

and therefore it shouldn't be a problem for most of the aplications.

Electrical bandwidth of the photodetecor for a laser source CoBrite DX4 (frequency tune range = ± 12 GHz) and 30 Hz modulation as an example:

$$BW_{el} = \frac{2\, R_{\max}\, \gamma}{c} = \frac{2\, R_{\max}\, f_{\text{BW}}}{c\, T_{\text{mod}}} = \frac{2 \cdot 100 \cdot 24 \cdot 10^9}{3 \cdot 10^8 \cdot 30} = 533.33 \text{ Hz} \tag{2.15}$$

Another method (proposed in [29]) is using balanced detector to measure the frequency directly instead of calculations from phase-shift. This allows for instantaneous frequency measurement with fast sweep rate.

2.3.2 Lock-in amplifier

Lock-in amplifier utilises homodyne detection. Lock-in amplifier is able to extract only the signal with exact frequency while other frequencies are

strongly attenuated. When a sinusoidal received signal is multiplied by the reference sinusoidal signal and integrated, it results in a non-zero value only when they are at the same frequency. Therefore it is frequency and also phase sensitive. They usually use mechanical optical chopper on the transmitter side. Originally lock-in amplifiers were developed with analog components (mixer and RC low-pass filter) on the receiver side but nowadays they exist in a form of digital signal processing (DSP) running on FPGAs.

The output is an integrated DC value (amplitude only). Sometimes dual-phase demodulation is used which requires both sine and cosine component and enables amplitude and phase measurements and advanced postprocessing (usually FFT).

Lock-in amplifier has not been studied for LiDAR use. The only mention is in the article [30] where it is used for distance measurement (simulated by optical fiber) and also for velocity and displacement measurements. But the setup is too complicated, consisting of big and expansive discrete components as shown in Fig. 2.5. Using lock-in amplifier to enhance LiDAR range is difficult because it is sensitive to phase which cannot be predicted for random objects. Another disadvantage is the need for averaging which makes measurements slow and not suitable for scanning LiDARs but it could be utilised for optical power measurements. The ideal input would be a perfect sine wave which is also hard to achieve.

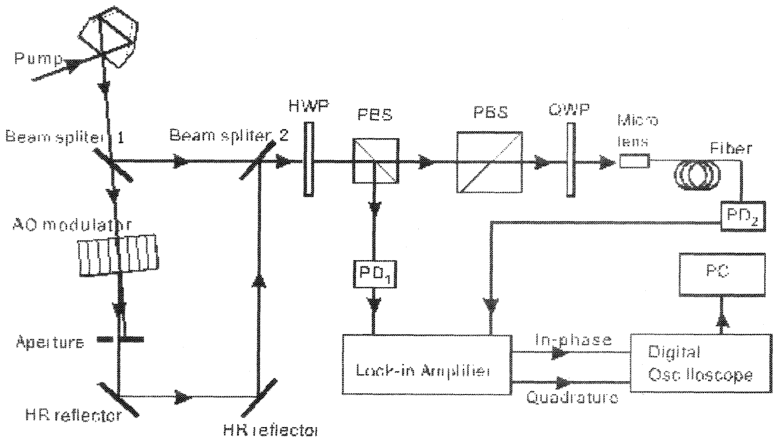

Figure 2.5: Experimental setup for distance measurement with lock-in amplifier, from [30]. Components: acousto-optical modulator (AOM), polarization beam-splitter (PBS), half-wave plate (HWP), quarter-wave plate (QWP), photodiode (PD).

Chapter 3

Experimental part

This chapter presents designed setups of particular LiDARs, realisation of those setups, their testing, measurements with them and evaluation of gathered results. The main goal is to compare time of flight and amplitude modulation methods on different setups. Mainly the capability to measure the distance correctly is evaluated. Three different experimental setups are designed throughout this chapter. The main focus is on functionality, range resolution improvement and simplicity in terms of cost and availability of components. Those setups are all built in the optical laboratory and they are all evaluated with measurements and data processing MATLAB scripts. This chapter is divided into sections starting from the simple setup that was designed as a proof of concept to more advanced setups.

3.1 The optical fibre setup

3.1.1 Design

Firstly optical fibre setup was designed as a proof of concept for amplitude modulated LiDAR. Having setup consisting of optical fibre components makes beam alignment much easier. Its purpose is to evaluate the idea of determining the length or distance by measuring a time offset between two sine waveforms (Reference captured directly at the source and the received signal). This setup could be described as an optical fibre length measurement device but

the concept is a great proof of concept for LiDAR as further shown. The measured time delay is varied by change in length of an optical fibre. The length of fibres could be measured by the amplitude modulation method and also by the time of flight for comparison. This setup and its description are shown in Fig. 3.1. One of the key components is an intensity/amplitude modulator which is driven by a modulation signal from a signal generator and which modulates the continuous light beam from a laser. After the optical fibre under test there is a receiving photodiode. RF signal from a PD and a reference from a signal generator are acquired on an oscilloscope.

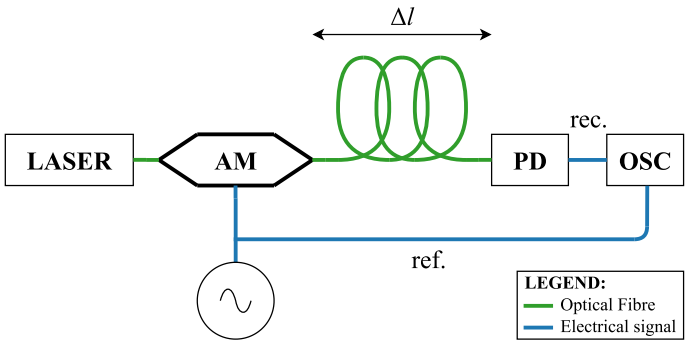

Figure 3.1: The optical fibre setup with a laser source and Amplitude Modulator (AM) at the transmission side. Signal generator that provides the RF signal to the AM is marked by a sine wave (∼). Optical fibre is to be changed for different lengths that are measured. Receiving end consists of a photodetector (PD) and an oscilloscope (OSC) for data acquisition. Received signal shown as "rec." and reference signal is "ref.". Fibres with different length Δl can be examined.

3.1.2 Components

Optical components, measurement devices and laboratory equipment that were used for the setup in this section are described here. The data were observed and acquired with the oscilloscope (OSC) Keysight MSOS104A and InfiniiumWaveform [31] and processed with MATLAB on a PC. The sine wave was reconstructed with the sineFit [32] add-on. Other devices used for experiments (with symbols used in schematic diagrams):

- PD | Photodiodes: ThorLabs PDA10CS (adjustable gain) and PDA CF-EC
- ∼ | Waveform generator: T3AWG3252
- LASER | Tunable laser: CoBrite DX4
- AM | Amplitude modulator: ThorLabs Covega Mach-10 081
- Power supply: AIM-TTI PL303QMD-P
- Power meter: ThorLabs S122C head and PM100D console

- ThorLabs kinematic mounts, posts and holders
- SMF-28 optical fibres with different lengths and with FC-APC connectors

3.1.3 Measurements

Based on the schematic design a measurement setup was built, see Fig. 3.2. This setup was used to prove that the suggested concept of using an amplitude

(a) : A closeup photo.

(b) : Photo off all components and devices, only signal generator and laser source are off the shot. Laser is connected to the intensity modulator. Optical fibres of which the length is measured follow. The end is connected to the photodiode. Electrical signal from the PD goes to the oscilloscope where the reference signal from signal generator is also shown.

Figure 3.2: Two views of the optical fibre setup.

modulation for LiDAR works. Amplitude modulated signal gives an advantage of measuring time between transmission and reception of the signal. The modulated sine wave could be reconstructed from the original signal. A sine wave can be reconstructed from a low number of samples and therefore a

high sampling frequency was not needed as opposed to ToF LiDAR. It is also possible to reconstruct the sine shape very precisely which results in a higher resolution opposing the single pulse. The reference wave and reflected wave are compared in the time domain. In the example shown in Fig. 3.3 time delay is calculated from two time stamps captured at peaks of those sine waves and that allows for precise distance calculation (see Eq. 3.2). Results are summarised in Tab. 3.1 with comparison between four modulation frequencies.

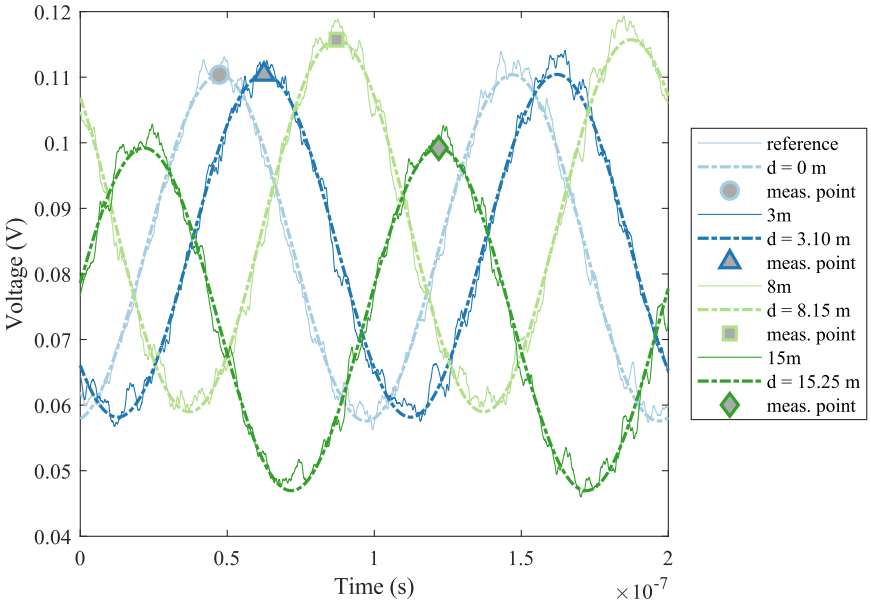

Figure 3.3: Distance measurement results for amplitude modulation with the optical fibre setup. Signal is approximated to sine form (indicated by dash-dotted curve). Modulating frequency is f=10 MHz. Data for these signals are emphasised in bold in Tab. 3.1).

The data for lower frequency modulation have bigger deviations (as promoted by statistics in Tab. 3.1). Using a 30 MHz modulation frequency results in a 1.16% mean error which is superior to a 1 MHz measurement with a 3.69% error. Therefore a higher frequency modulation was used to validate the data with more precision and better distance resolution. But higher frequencies offer a very short range as shown in Tab. 3.2. Lower frequency sine wave peaks are therefore used to calculate the approximate position for higher frequency peaks which are determined as peaks with the closest distance to lower frequency ones. This approach is illustrated in Figures 3.4 and A.1 and the following function was used to find the correct peak corresponding to the time delays measured for lower frequency signal ($\vec{t}_{\mathrm{LF}}$)

$$t_{\min} = \min(|\vec{t}_{\mathrm{LF}} - (\vec{t} - t_1)|), \tag{3.1}$$

Table 3.1: Results for AMCW measurements with the optical fibre setup. Data in bold correspond with signals shown in Fig. 3.3.

f_{mod} (MHz)	Distance d (m)		Measurement error		
	Expected	Measured	Error (%)	Mean	STD
1	3	*2.70*	9.97	3.69	3.95
	8	*7.92*	0.95		
	15	*15.02*	0.15		
4	3	2.83	5.67	2.83	1.76
	8	7.87	1.63		
	15	14.82	1.20		
10	3	**3.10**	3.33	2.29	0.74
	8	**8.15**	1.88		
	15	**15.25**	1.67		
30	3	*3.01*	0.30	1.16	0.62
	8	*8.12*	1.50		
	15	*15.25*	1.69		

where $\vec{t}$ is an array of timestamps of all peaks of the sine wave while t_1 is the first peak. Those two mentioned Figures show the difference in distance measuring precision between lower and higher frequencies, measured distances (in italic font in Tab. 3.1) support the idea that higher frequency allows increase in accuracy. This method of combining two frequencies (1 and 30 MHz) allowed a great precision of 1.16% but also outstanding theoretical range up to 300 m in free space (Tab. 3.2).

The maximal range of this approach is given by the modulation signal period ($T = \frac{1}{f}$) and speed of light in an optical fibre (v_{fib}). Equation for 1 MHz modulation signal as an example would be

$$d_{\max} = v_{\text{fib}} \frac{T}{2} = \frac{c}{n_{\text{eff}}} \cdot \frac{1}{2\,f} = \frac{3 \cdot 10^8}{1.468} \cdot \frac{1}{2 \cdot 1 \cdot 10^6}\ \text{m} = 102.18\ \text{m}, \tag{3.2}$$

where n_{eff} is the effective refractive index for SMF-28 at 1550 nm. The range is approaching 300 m in free space. This is calculated for other frequencies in Tab. 3.2. The same approach is used to calculate the estimated distance from two timestamps of sine peaks of measured data (see Eq. 2.6).

Table 3.2: Maximal theoretical range of a AMCW LiDAR based on its modulation frequency.

f_{mod} (MHz)	Maximum distance d (m)	
	in optical fibre	in free space
1	204.36	299.79
4	51.09	74.95
10	20.44	29.98
30	6.81	9.99

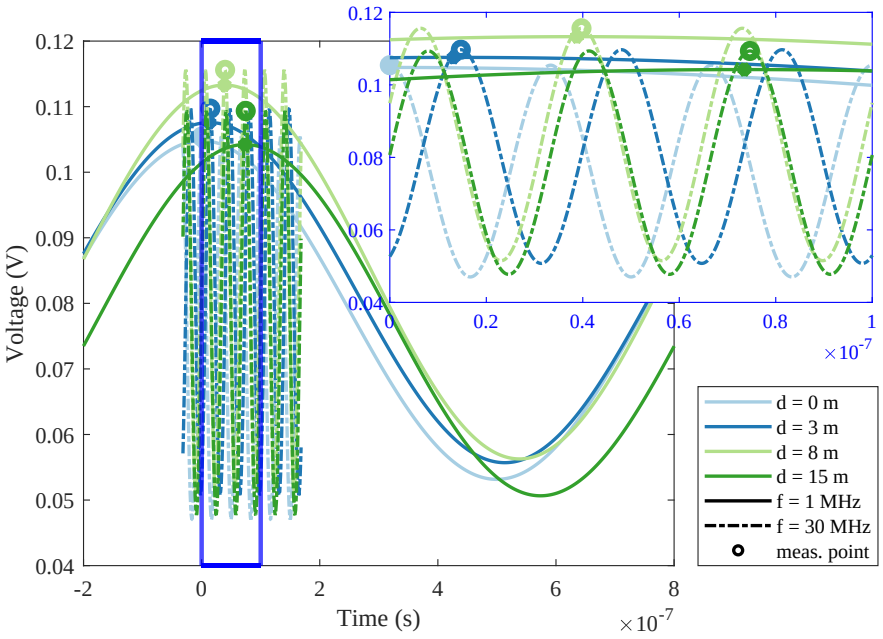

Figure 3.4: Distance measurement results for amplitude modulation with the optical fibre setup. Zoomed time scope is shown in the blue graph, zoom area is bordered by the blue rectangle. Signal is approximated to sine form. Measured with frequencies f=1 MHz as reference with a long range capability and for f=30 MHz with better resolution. Position of a lower frequency peak determines which is the correct peak in a higher frequency signal. Points where timestamp was taken shown as circles. Peak of the reference signal shifted to 0 s position. Measured distances corresponding to this graph are highlighted in italic in Tab. 3.1.

These measurements proved that the amplitude modulation for LiDAR is a functional concept. Achieving both good resolution and good range is possible with the combination of two modulation frequencies. The main reason for minor inconsistency of the data is precision with electrical triggering when data acquisition is made. Another aspect bringing error into calculations is the sine function approximation and therefore correctness of the peak position. This measurement was done with 20 GHz sampling rate which is not available with cheaper electronics and therefore data clarity would be decreased.

3.2 The free space setup

3.2.1 Design

The free space experimental setup is based on the first one presented in Section 3.1. There were multiple options for designing this setup as discussed in this paragraph. Reference signal is required for accurate distance measurement. The distance would be calculated from the time delay between the reflected signal and this reference. Two options to produce a reference beam to measure the time of flight exist. First possibility is to put an optical beamsplitter (BS) in the beginning of the optical path. Second one is to use a fibre circulator which is more convenient in terms of alignment but it adds optical path to the signal which needs to be subtracted. There are also multiple ways to receive the reflected signal in a LiDAR system. One is to collimate it back into the source fibre (monostatic LiDAR), later separate it with fibre beamsplitter or circulator and to receive it on the photodiode. Other option would be to receive into a photodiode or into the second collimator indirectly in a different point in space as close as possible to the transmitting collimator (bistatic LiDAR). This is more complicated for alignment and the setup needs to be calibrated either for a shorter or a longer distance due to alignment errors. In each case at least two photodiodes are used in two optical paths to capture both reference signal at the time of transmission and the actual reflected signal.

As a result of this discussion the free space setup was designed as shown and described in Fig. 3.5. Evaluation of measurement methods could be conducted in a more realistic environment with this setup. This LiDAR was designed to be built on an optical table for severe stability. It was designed as a fibre based LiDAR which has an advantage of easy alignment but the final (measured) optical path is collimated from fibre to free space. Continuous laser light is modulated by an amplitude modulator, transmitting path is separated at a circulator, reference signal is decoupled at a beamsplitter and light is then collimated from a fibre into the free space. Highly reflective target could be placed into different distance from the LiDAR for measurements. Reflected signal is later focused back to the fibre and directed towards a receiving photodiode by a circulator.

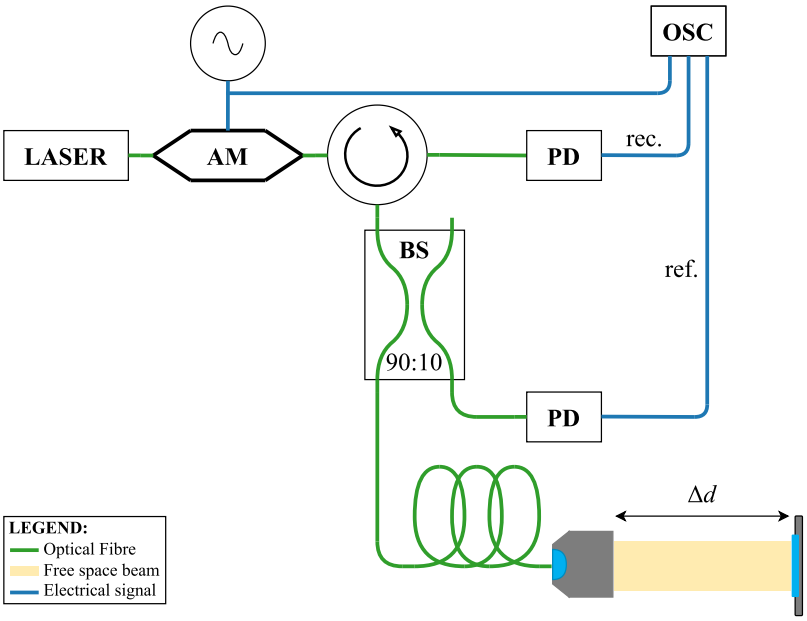

Figure 3.5: The free space setup where the laser source is amplitude modulated by amplitude modulator (AM). Circulator (↻) is used to separate transmitted and received signals and a second PD behind a beamsplitter (BS, 90:10) is used for capturing a reference signal. Light is transferred from a fibre to the free space with a fibre collimator. Distance Δd from the mirror target is measured.

The advantage of this designed setup is that it can be used for both ToF and AM LiDARs and therefore those methods can be directly compared. Only a change in a laser modulation is needed. Therefore the used amplitude modulator should be able to modulate both sine and rectangular pulse signals. This design is transferred into the real setup and evaluated in the next sections.

3.2.2 Components

Following components and devices were used for this particular setup:

- PD | Photodiodes: ThorLabs PDA10CS (adjustable gain) and PDA CF-EC
- ∼ | Waveform generator: T3AWG3252
- LASER | Tunable laser: CoBrite DX4
- AM | Amplitude modulator: ThorLabs Covega Mach-10 081
- ↻ | Circulator: ThorLabs 6015-3-APC

- Collimator: ThorLabs F810APC-1550
- Beamsplitter: ThorLabs coupler (SM, 2x2, 90:10, 1550 nm)
- Mirror: ThorLabs PF10-03-P01 ($R_{\text{avg}} > 97.5\%$ for 450nm - 2μm)
- Red laser source: ThorLabs HLS635 (635 nm)
- Power meter: ThorLabs S122C head and PM100D console
- Power supply: AIM-TTI PL303QMD-P
- ThorLabs kinematic mounts, posts and holders

3.2.3 Preparation of the setup and alignment

The setup was built according to previous design ideas in previous section and devices were chosen to match the specified aim. One of the important criteria was bandwidth which could be a limiting factor for photodiodes, waveform generators, modulators and also for an oscilloscope. The aim was to capture a signal of 32 MHz at maximum and that was a reason to use PDA CF-EC and sacrifice the adjustable amplifier ability of PDA10CS which only has a 17 MHz BW. Also the correct setting for all applicable devices needed to be set, especially the oscilloscope's possibilities for bandwidth limiting and bandpass filtering were turned off. The Intensity modulator was biased with +5V DC to lock the operating point at fixed position to maximise the modulation intensity and to prevent drift of the modulator. The laser was set for 1500.001 nm wavelength and 6 dBm power.

Alignment of components is one of the most critical but also time consuming operations in free space optics and therefore in any LiDAR setup. It is crucial to align all components to allow for transmission of most power into the correct direction. The longer the range is, the smaller angle shift is allowed at the transmitting and receiving part. That was a reason why the first setup was done purely in optical fibres and then the free space still included some optical fibre components. All free space components were placed on an optical bread-board and mounted with clamps and posts. Two 2-axis micro-movement stages were used for precise positioning. The alignment procedure explained in the following paragraph was used for this setup but also for the setup presented next as the idea applies to alignment generally.

The setup was aligned according to the following methodology to capture all reflected power. Firstly a visible red laser was used to roughly align the setup visually. Then the collimator was positioned to shoot into the direction of the target mirror. Next step was to rotate the mirror to reflect directly back to the collimator. We observed the beam visually and tried for the best focus of the beam back to the fibre. Secondly we connected the setup to the

laser source at the final wavelength (1550 nm) and used an optical power meter to find the correct alignment, being one with the highest possible power at the output. This was tricky especially because focusing light back from free space into the fibre needs a lot of precision.

3.2.4 Measurements

Experiments in free space were made after the proof of concept (Section 3.1) was successful. Following measurements test this method in a more realistic environment. The setup was almost identical to the designed schematic as can be seen in Fig. 3.6.

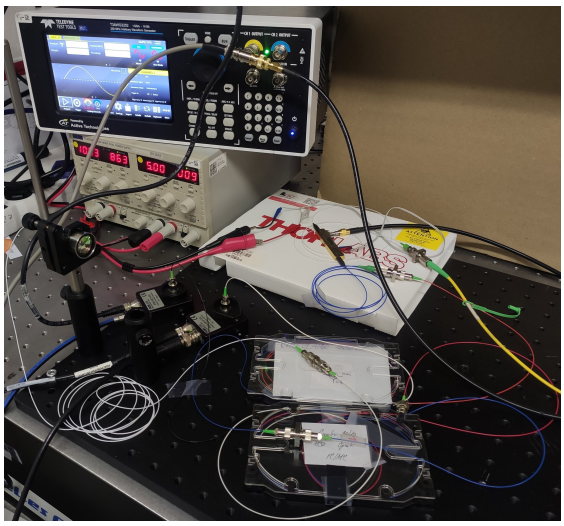

(a) : The amplitude modulator in the centre is biased by a laboratory power supply and driven from a signal generator. On the left there is a collimator which collimates light from fibre into the free space. Fibre beamsplitter, circulator and two photodiodes can be also seen in the bottom.

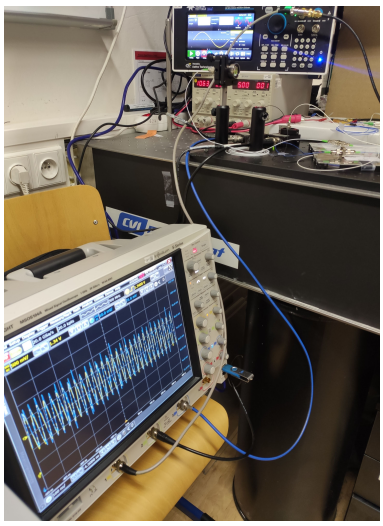

(b) : View of the setup with the oscilloscope in the foreground. Channel 1 is a reference from the signal generator, ch. 2 is the actual signal after the circulator and ch. 3 is a reference from a beamsplitter.

Figure 3.6: The free space setup built in a laboratory.

Time of flight measurements

The setup was firstly evaluated with a time of flight method. Two distances were measured in the free space. Distance was calculated by the following equation (based on Eq. 2.1) where the extra path (d_{fib}) in optical fibre is

subtracted

$$d = \frac{c\,(t - \frac{d_{\text{fib}}}{v_{\text{fib}}})}{2} = \frac{3 \cdot 10^8\,(5.16 \cdot 10^{-8} - \frac{8.12}{2.04 \cdot 10^8})}{2}\ \text{m} = 1.78\ \text{m}, \tag{3.3}$$

where t is the measured time delay between the signals. The measured time of flight data are demonstrated in Fig. 3.7. In the following section same distances are measured with amplitude modulated signal and with an improvement to the data processing to mitigate the path in an optical fibre.

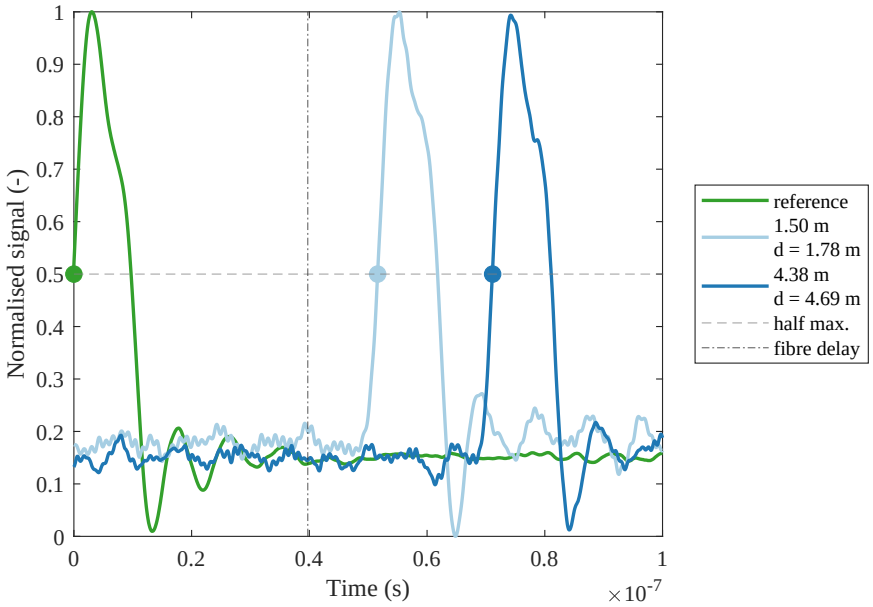

Figure 3.7: Time of flight measurements for pulsed signal with frequency of 1 MHz and 1% duty cycle (10 ns pulse). Measured on the free space setup. Two distances (with measurements points at half maximum) are shown with reference point on a photodiode and calculated reference point (vertical dash-dotted line) after subtraction of delay in an optical path through optical fibre as calculated in Eq. 3.3. All signals are normalised for better clarity in the graph.

Amplitude Modulation measurements

Amplitude modulation was selected as it should bring better resolution and possibilities for more precise data processing according to the theoretical analysis. In Fig. 3.8 measured amplitude modulation results are shown in contrast with ToF from Fig. 3.7. The ToF and AMCW results are clearly not matching the tape measured distances. There is a certain distance for a beam to travel to a reference photodiode in an optical fibre where lengths were measured only approximately with a tape measure. Therefore there is an offset added to the data. Mean offset was calculated and equals 0.34 m.

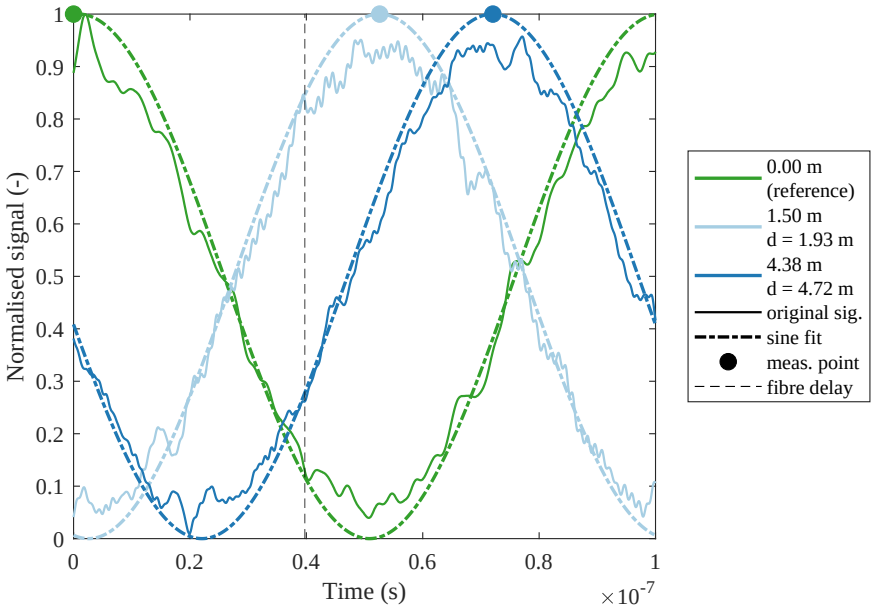

Figure 3.8: Distance measurements for amplitude modulation with a reference point on a photodiode and a calculated reference point (vertical dashed line) after subtraction of a delay in an optical path through an optical fibre. Measured on the free space setup. 10 MHz amplitude modulated signal is approximated to a sine curve. Both original data and the sine fit are normalised. Two distances from reference point are shown. In the legend, tape measured distance is shown and the LiDAR calculated distance is bellow.

After subtracting this offset (see rows designated "(offset=-0.34 m)" in Tab. 3.3) the results are precise with mean error of 2.34% and 3.00% for ToF and AMCW respectively. This way of conducting measurements is not always repeatable and a better procedure is to calibrate the data. For that it is needed to measure the distance for target in a zero position. In Fig. 3.9, calibrated measurements are shown. For that the reflecting mirror target was put directly at the collimator. The measured time delay for this 0 m measurement was then subtracted from measurements for other distances. This is a very precise method and it doesn't involve taking into account a length of a path towards a reference PD through an optical fibre as previous measurements needed to do because it is subtracted. Graphs graphs for another two frequency samples are also included in Appendix A to show why 10 MHz frequency was optimal for this measurement as it provides optimal range and most precise results. Resulting measured distances have a great precision of 2% and less. An advantage over ToF data (Fig. 3.7) and over uncalibrated measurements is clearly visible in Tab. 3.3.

Table 3.3: Measured values on the free space setup and a comparison between methods. Calculation of the distance is done according to Eq. 3.3 where an example of a time of flight calculation is shown for 1.5 m. ToF and AMCW have an offset due to an incorrect estimation of the length in optical fibre towards reference PD. Mean of this offset is calculated and subtracted in the succeeding rows. Lastly AMCW results with calibration for 0 m are shown.

Method	Distance d (m)		Measurement error		
	Expected	Measured	Error (%)	Mean	STD
ToF	1.50	1.78	18.67	12.87	5.79
	4.38	4.69	7.08		
ToF (offset=-0.34 m)	1.50	1.44	4.00	2.34	1.66
	4.38	4.35	0.68		
AMCW	1.50	1.93	28.67	18.21	10.45
	4.38	4.72	7.76		
AMCW (offset=-0.34 m)	1.50	1.59	6.00	3.00	3.00
	4.38	4.38	0.00		
Calibrated AM	1.50	1.47	2.00	1.11	0.89
	4.38	4.39	0.23		

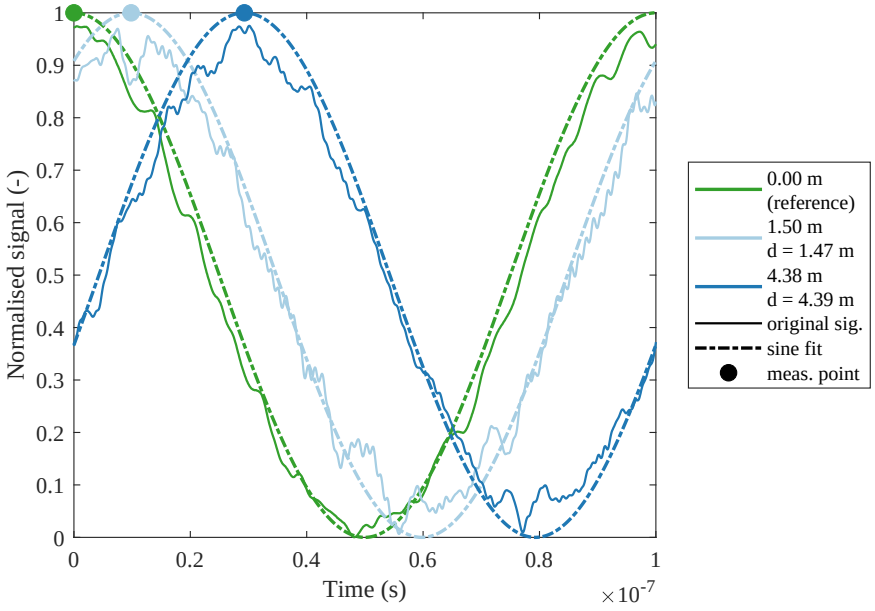

Figure 3.9: Distance measurements for amplitude modulation with a calibrated reference. Measured on the free space setup. 10 MHz amplitude modulated signal is approximated to sine curve. Both original data and sine are normalised. Two distances from reference point are shown. In the legend, tape measured distance is shown and LiDAR calculated distance is bellow. Two similar measurements done with different modulation frequencies are displayed in Figures A.2 and A.3.

Other measurements were made in free space again but with a changed setup. There are measured signals with a reference point being taken directly after a collimator where a reference beam was separated at the beamsplitter. This would have worked better if a photodiode for capturing the returned signal was placed also in the free space on the other side of a beamsplitter with distances being the same (as pictured in Fig. 3.10 and analysed in the following sections). Otherwise another calibration or subtraction of some time delay would be needed as debated earlier. Therefore those data are only shown in Appendix in Fig. A.4 and they apparently integrate the error of the uncertain length of path in an optical fibre.

Measurements with the free space setup showed the principle of the ToF and AMCW LiDARs. Very good precision was achieved with proper calibration of the setup. Calibrated AMCW beats the traditional ToF method.

3.2.5 Data processing

The data processing was a very important part of all conducted measurements not only in this section. After data are acquired they also need to be processed to calculate relevant outcomes. As the goal of most LiDAR systems is to calculate distance from a time delay between two signals my first focus was on establishing a sampling point for getting a time stamp for those signals. For time of flight measurements we decided to work with the pulses in their original form and we chose a first point where signal got over its half maximum as a time stamp because a shape of this signal was distorted from its original rectangular form and searching for its maximum point would not be as precise (measurement point are visible for example in Fig. 3.7). A different method for amplitude modulated signal was selected. Firstly the data were fitted with a sine wave fit and a peak of this fit was found (this sine fit and assigned peaks are depicted for example in Fig. 3.8). This method makes it very good for noise rejection because the fit takes into account all signal's fluctuations. But it's downside is that it takes a certain time for processing of this signal. That is making it more complicated for real time applications because high processing power would be required. A method of combining two modulation frequencies to achieve better resolution and range (see Fig. 3.4) was also supported by the programmed script. In general, results of this data processing could be seen in all tables and figures throughout this chapter.

3.3 The improved free space setup

3.3.1 Design

The improved free space setup was designed based on previous experience. This setup (shown in Fig. 3.10) suggests capturing reference signal straight after the beam collimator to eliminate calibration and increase precision of an uncalibrated setup. Two photodiodes in free space are used for both

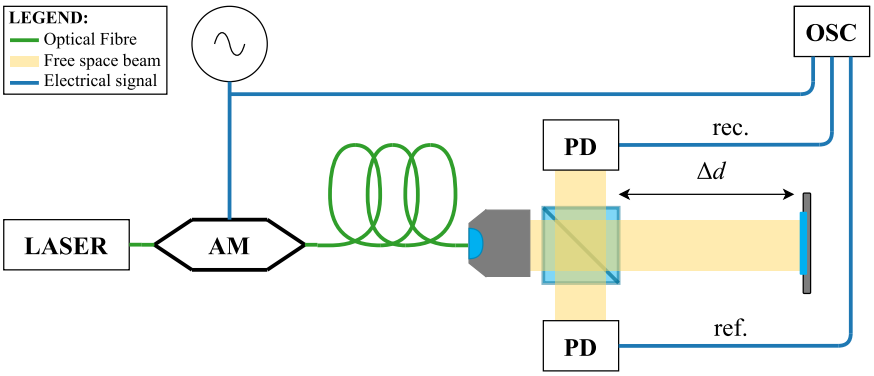

Figure 3.10: The improved free space setup where the laser source is again amplitude modulated. Beamsplitter in a free space is used to separate reference light beam into first photodiode and then capture a reflected beam into a second receiving photodiode. Mirror is shown as a target to evaluate this design but less reflective targets can be measured as the sensitivity should be improved here.

transmitted signal reference and received signal capturing with a single beamsplitter (two-way mirror) to divide the beam. The biggest advantage of this setup is no need for calibration. The resulting distance can be calculated directly from the time delay between transmitted beam on a reference PD and received signal on the receiving PD.

3.3.2 Components

Following optical components, measurement devices and laboratory equipment were used for this final setup. The data were observed and acquired with oscilloscope Agilent InfiniiVision MSO7104B and processed with MATLAB on a PC. Other devices used for experiments:

- Photodiodes: EOT ET-3000TTL, ThorLabs DET10A/M

- Laser driver and pulse generator: Picolas LDP-V 50-100 V3.3 and Picolas PLCS-21 with soldered laser diode (905 nm, 10° divergence)
- Power supply: Toellner TOE 8952
- Power meter: ThorLabs S132C head and PM100A console
- Beamsplitter cube: ThorLabs BS023 (70:30, 700-1100nm)
- Lenses: ThorLabs Ø25.4 mm: ACL25416U-B ($f_o = 16$ mm), ACA254-030-B ($f_o = 30$ mm)
- ThorLabs kinematic mounts, translation stages, posts and holders

3.3.3 Measurements

Only the time of flight method was used to evaluate this final setup with regard to availability of usable components and eye safety. The idea was to use pulsed laser source to achieve a low continuous power but a high pulse power to be able to measure less reflective targets. A retro-reflective tape was chosen to represent a target. The final setup differs a little from the originally designed setup as it uses laser driver (with included pulse generator) with soldered laser diode and no fibre components. Diagram in Fig. 3.11 illustrates this difference. This setup as it was built is pictured in Fig. 3.12.

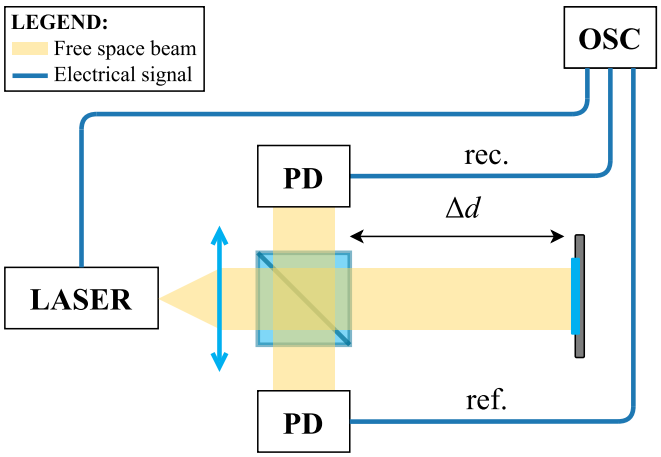

Figure 3.11: Schematic of the improved free space setup as it was built. It differs from the design idea (Fig. 3.10) by eliminating the fibre components and using a soldered LD directly onto a laser driver with a pulse generator module. Converging lens (↕) is used to collimate light.

Important part of the built of this setup was choosing a correct collimating lens at a transmitting side and focusing lens at a receiving end. We searched for a shortest focal length ($f_o = 16$ mm) to have a narrow collimated beam to

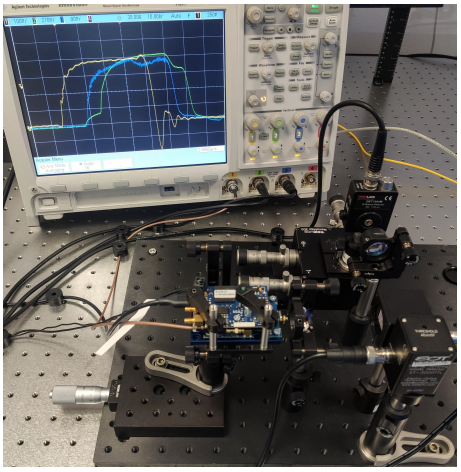

(a) : Transmitting and receiving part with laser driver, BS and two PDs. Signals are shown on the oscilloscope, yellow is a current monitor on a LD, blue is from a reference PD and green is the reflected signal of a target.

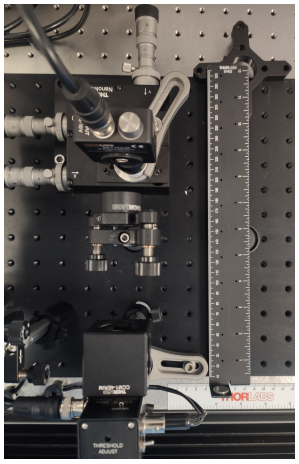

(b) : Closeup on a BS, reference PD and a receiving PD. Receiving PD is placed on a 3-axis translation stage and the lens is mounted to a tip-tilt stage for alignment. A ruler is shows distances of PDs.

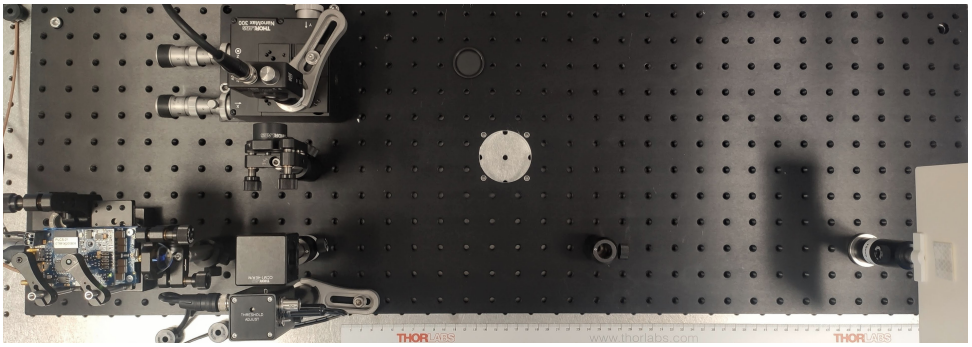

(c) : Top view of the whole setup. Tape measure is present for measurement evaluation. The laser driver with a soldered LD is on the left followed by a beamsplitter, receiving PD is at the top, reference PD is at the bottom and the target is on the right.

Figure 3.12: Three different views of the improved free space setup.

reach as high power as possible in a small diameter (d). The resulting beam diameter was calculated thanks to ray optics and trigonometry

$$\tan(\vartheta) = \frac{d/2}{f_o} \longrightarrow d = 2 \cdot f_o \cdot \tan(\vartheta) = 2 \cdot 16 \cdot \tan(10^\circ)\ \text{mm} = 5.65\ \text{mm} \quad (3.4)$$

where $\vartheta = 10^\circ$ is a divergence angle of a used LD. Settings for the laser driver were 50 ns pulse width and 50 Hz repetition rate at a current of 7 A (voltage drop on the LD was around 4.7 V according to previous evaluation measurement). The measured optical power of a collimated beam as an average over 4 distances was 2.85 μW continuous and 1.14 W in a pulse.

Data were measured with averaging of 8 samples (pulses) for better precision. Signal was triggered by the rising edge of a LD's current sensing. Receiving

photodiode was 105mm further than the reference photodiode and therefore this delay was subtracted ($d = \frac{ct-0.105}{2}$) in a similar way to Eq. 3.3. Results are pictured in Fig. 3.13 and in Tab. 3.4. As can be seen from those measurements this method is precise to 5%. This can be blamed on human error in tape measuring the distances (tape measure used is pictured on the bottom of Fig. 3.12c. The used beamsplitter was not designed for such low sensitivity application and it's internal reflections caused too much noise on the detector when higher power was needed. Those reflections can be seen in the graph, especially for longer distances. Range of 2.80 m was also measured but the reflections exceeded the half maximum threshold and therefore the measurement was not successful.

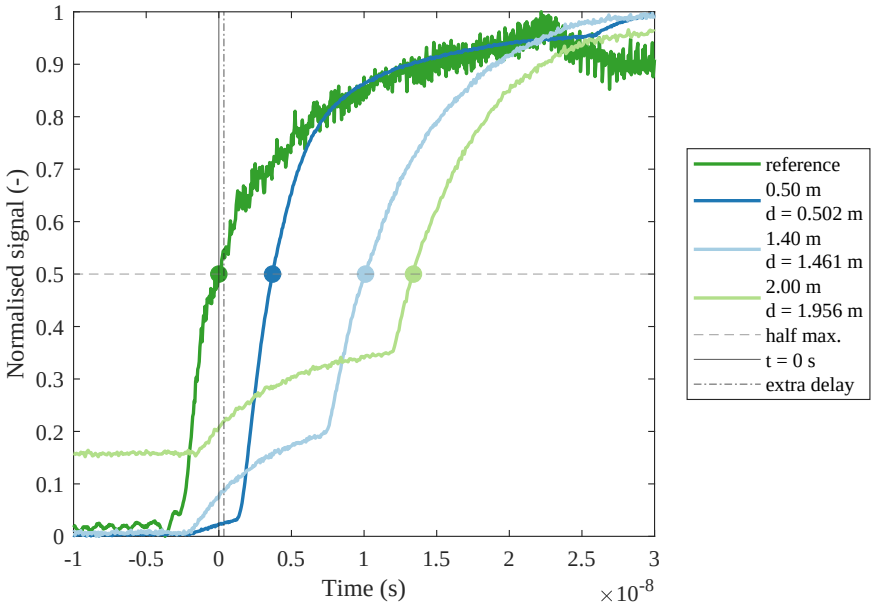

Figure 3.13: Time of flight measurements for pulsed signal with 50 ns pulse width and 50 Hz repetition rate. Measured on the improved free space setup. Three distances (with measurements points at half maximum) are shown with reference point on a photodiode and calculated reference point (vertical dash-dotted line) after subtraction of short difference in distance between reference and receiving PDs (*extra delay*). All signals are normalised for better clarity in the graph.

Table 3.4: Results for ToF measurements with the improved free space setup.

Method	Distance d (m)		Measurement error		
	Expected	Measured	Error (%)	Mean	STD
ToF	0.500	0.502	0.42	2.33	1.63
	1.400	1.462	4.39		
	2.000	1.956	2.19		

This setup offered an increased sensitivity as it was able to detect a retro-reflective target. However it did not offer desired improvements because of limitations on a beamsplitter. A beamsplitter with better performance (with some anti-reflective coating and made of more pure materials) would be a good option in further extension of these measurements. This setup has also proved that it is theoretically possible to have a setup without needing a calibration. But it could not be done to avoid the subtraction of extra length because of space limitations and therefore the suggested advantage was not achieved. Although it is outside of a scope of this thesis, we believe that the measured accuracy of 2.33% can be further improved with innovations like upgraded beamsplitter or matched distance between beamsplitter and both photodiodes.

Chapter 4

Conclusion

This thesis studied LiDARs in general, their components, applications and also specific aspects of the LiDAR development. Theoretical part was focused on searching for a method to increase LiDARs' sensitivity. Especially time of flight, amplitude modulation and coherent methods were studied. Frequency modulated coherent LiDAR is the most sensitive on paper but also very complex because sophisticated and costly equipment is needed. ToF and AMCW methods also offer outstanding performance in certain applications and are easier to implement.

In the practical part, ToF and AMCW LiDARs were designed, built, measured and evaluated. Firstly, the optical fibre setup was designed and built. It showed that using AMCW is feasible and that it is possible to achieve a mean error of 2.29% in distance measurement with a range up to 30 m. Then a method to combine two AMCW modulation frequencies was proposed. This allowed for increased range while also increasing resolution. Theoretical range of up to 300 m can be achieved while maintaining a low average error of 1.16% as showed in calculations and measurements. Secondly, a different setup was built to measure in the free space. Time of flight method was utilised with mean error of 2.34%. Measurements with AMCW followed and resulted in an 3.00% error. Based on this experience, calibration was suggested. Calibrating for the zero distance heavily helped to improve the results. Calibrated AMCW setup achieved a 1.11% error and therefore it outperformed the traditional ToF method. Also several signal processing methods for the AMCW LiDAR were shown with different procedures to analyse and calculate the distance. Improved SW allowed us to evaluate the exact phase shift between transmitted and received signals. This led to improved precision and overall better performance of the built LiDAR.

Doing a calibration is not always simple and therefore a redesigned setup that would mitigate the need for calibration was designed and later built. This setup was also built to be much more sensitive and it was able to measure reflections from retroreflective surfaces. This setup was evaluated with a time of flight method. A beamsplitter was needed to provide a reference signal. Internal reflections inside a beamsplitter were a challenge as they added a noise on a receiver. This was a limiting factor to achieving higher sensitivity or longer distance. Average accuracy of 2.33% show a big potential of this setup and we suggest further work extending on this idea. Beamsplitter with a better performance (especially in reducing internal reflections) would be needed. Possibility to further extend on the topic of this thesis is to conduct measurements with the bistatic LiDAR where sending and receiving paths are offset and not collinear as in our setup. Also the idea of combining two modulation frequencies is an interesting topic for future work.

Bibliography

[1] National Research Council, *Laser Radar*. Washington, D.C: National Academies Press, 2014-03-14. [Online]. Available: https://doi.org/10.17226/18733

[2] P. F. McManamon, *LiDAR technologies and systems*. Bellingham, Washington, USA: SPIE Press, [2019].

[3] V. Molebny, P. McManamon, O. Steinvall, T. Kobayashi, and W. Chen, "Laser radar," *Optical Engineering*, vol. 56, no. 3, 2017-03-01. [Online]. Available: http://opticalengineering.spiedigitallibrary.org/article.aspx?doi=10.1117/1.OE.56.3.031220

[4] A. Campbell. (2022) Introduction to electromagnetic spectrum. Washington DC, USA. [Online]. Available: https://www.nasa.gov/directorates/heo/scan/spectrum/overview/index.html

[5] Jimmy Westberg, "How to create a electromagnetic spectrum using pgfplots package (together with colormaps)," Hudiksvall, Sverige, 2017. [Online]. Available: https://tex.stackexchange.com/a/348492

[6] (2001- 2022) File:atmospheric transmission.png. San Francisco (CA). [Online]. Available: https://commons.wikimedia.org/wiki/File:Atmospheric_Transmission.png

[7] *IEC 60825-1:2014*, 3rd ed., 3 rue de Varembé, 1211 Geneva 20, Switzerland, 2014.

[8] P. McManamon, *Field Guide to Lidar*, 1st ed. Bellingham, Washington, USA: SPIE PRESS, 2015.

[9] Danh. (2001- 2022) File:laser class en 60825-1.en.svg. San Francisco (CA). [Online]. Available: https://commons.wikimedia.org/wiki/File:Laser_class_EN_60825-1.en.svg

[10] Han-Kwang. (2001- 2022) File:iec60825 mpe j nm.png. San Francisco (CA). [Online]. Available: https://commons.wikimedia.org/wiki/File:IEC60825_MPE_J_nm.png

[11] T. Kim, "Realization of integrated coherent lidar," Ph.D. dissertation, EECS Department, University of California, Berkeley, May 2020. [Online]. Available: http://www2.eecs.berkeley.edu/Pubs/TechRpts/2020/EECS-2020-38.html

[12] S. X. Li, "Apparatus, method, and computer program for a resolution-enhanced pseudo-noise code technique," US Patent 9 081 096, 2015.

[13] R. Paschotta. (2022) Fiber lasers versus bulk lasers. Frauenfeld, Germany. [Online]. Available: https://www.rp-photonics.com/fiber_lasers_versus_bulk_lasers.html

[14] L. Hofer. (2016) Cmos vs. ccd sensors and overview. Redding, CA, USA. [Online]. Available: https://dataray.com/blogs/dataray-blog/cmos-vs-ccd-sensors-and-overview

[15] B. D. Monte. (2010) Electron-multiplying ccd for lidar applications. Pittsfield, MA, USA. [Online]. Available: https://www.photonics.com/Articles/Electron-Multiplying_CCD_for_Lidar_Applications/a43365

[16] M. D. Turner, G. W. Kamerman, P. F. McManamon, P. Banks, J. Beck, A. S. Huntington, and E. A. Watson, "A comparison flash lidar detector options," *Laser Radar Technology and Applications*, vol. 2016, no. XXI, 2016. [Online]. Available: http://proceedings.spiedigitallibrary.org/proceeding.aspx?doi=10.1117/12.2229068

[17] Y. He and S. Chen, "Recent advances in 3d data acquisition and processing by time-of-flight camera," *IEEE Access*, vol. 7, no. 7, pp. 12 495–12 510, 2019. [Online]. Available: https://ieeexplore.ieee.org/document/8606938/

[18] (2022) Lidar for automotive and industrial applications 2021. Lyon-Villeurbanne, FR. [Online]. Available: https://s3.i-micronews.com/uploads/2021/09/YINTR21174-LiDAR-for-Automotive-and-Industrial-Applications-2021-Sample.pdf

[19] *SAE J3016*, 202104th ed., Warrendale, PA, USA, 2021.

[20] A. Reyes. (2021) Mercedes-benz wins world's first approval for level 3 autonomous cars: What's that mean? USA. [Online]. Available: https://www.slashgear.com/mercedes-benz-wins-worlds-first-approval-for-level-3-autonomous-cars-whats-that-mean-13702207/

[21] P. Sandborn. (2019) Fmcw lidar: Scaling to the chip-level and improving phase-noise-limited performance. Berkeley. [Online]. Available: http://www2.eecs.berkeley.edu/Pubs/TechRpts/2019/EECS-2019-148.html

[22] S. Royo and M. Ballesta-Garcia, "An overview of lidar imaging systems for autonomous vehicles," *Applied Sciences*, vol. 9, no. 19, p. 4093, 2019. [Online]. Available: https://www.mdpi.com/2076-3417/9/19/4093

[23] F. Villa, F. Severini, F. Madonini, and F. Zappa, "Spads and sipms arrays for long-range high-speed light detection and ranging (lidar)," *Sensors*, vol. 21, p. 3839, 06 2021.

[24] B. Behroozpour, P. A. M. Sandborn, M. C. Wu, and B. E. Boser, "Lidar system architectures and circuits," *IEEE Communications Magazine*, vol. 55, no. 10, pp. 135–142, 2017.

[25] H. W. Yoo, N. Druml, D. Brunner, C. Schwarzl, T. Thurner, M. Hennecke, and G. Schitter, "Mems-based lidar for autonomous driving," *E & i Elektrotechnik und Informationstechnik*, vol. 135, no. 6, pp. 408–415, 2018. [Online]. Available: http://link.springer.com/10.1007/s00502-018-0635-2

[26] J. P. Godbaz, M. J. Cree, A. A. Dorrington, and A. D. Payne, "A fast maximum likelihood method for improving amcw lidar precision using waveform shape," in *SENSORS, 2009 IEEE*, 2009, pp. 735–738.

[27] E. Canoglu. (2019) Lidar: A coherent vision for autonomous vehicle sensors (part 3). USA. [Online]. Available: https://www.neophotonics.com/coherent-lidar-self-driving-car/

[28] (1999-2022) Balanced amplified photodetectors with fast monitor output. Newton, New Jersey, United States. [Online]. Available: https://www.thorlabs.com/newgrouppage9.cfm?objectgroup_id=5201

[29] J. Yang, T. Yang, Z. Wang, D. Jia, and C. Ge, "A novel method of measuring instantaneous frequency of an ultrafast frequency modulated continuous-wave laser," *Sensors*, vol. 20, no. 14, 2020. [Online]. Available: https://www.mdpi.com/1424-8220/20/14/3834

[30] L. Li, S. Yang, X. Sun, L. Gao, L. Tao, C. Zhao, I. A. Shcherbakov, K. Xu, Q. Wang, A. V. Priezzhev, and V. I. Pustovoy, "Aom and lock-in amplifier lidar-radar system for distance measurement," *Event: Advanced Laser Technologies 2005, Tianjin, China*, pp. 63 443A–63 443A–7, 2005. [Online]. Available: http://proceedings.spiedigitallibrary.org/proceeding.aspx?articleid=1292237

[31] D. Gines, "Infiniiumwaveform toolbox," 2019. [Online]. Available: https://www.mathworks.com/matlabcentral/fileexchange/64705-infiniiumwaveform

[32] Y. Chen, "Sinefit," 2003. [Online]. Available: https://www.mathworks.com/matlabcentral/fileexchange/3730-sinefit

Appendix A

Figures

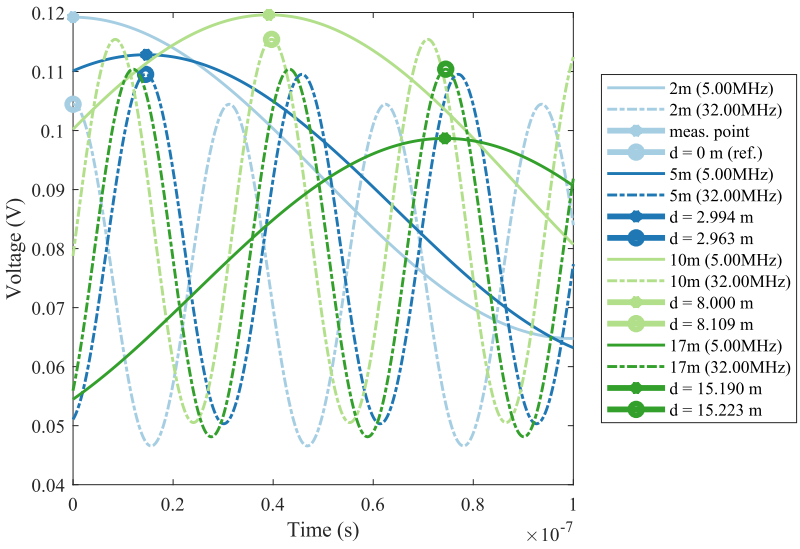

Figure A.1: Delay measurements for amplitude modulation. Signal is approximated to sine form for f=5 MHz as reference and for f=32 MHz with better resolution. Points where timestamp was taken shown as circles. Peak of the reference signal shifted to 0 s position.

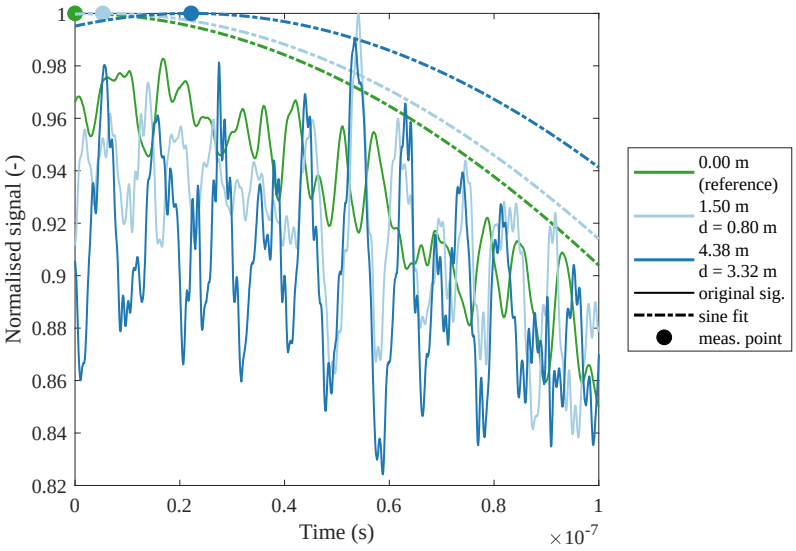

Figure A.2: Delay measurements for amplitude modulation with calibrated reference. 1 MHz amplitude modulated signal is approximated to sine curve. Both original data and sine are normalised. Two distances from the reference point are shown. In the legend tape measured distance is shown and LiDAR calculated distance is bellow. This graph suggests why distance measurement at this frequency is not very precise as noise on the original data doesn't allow for exact sine approximations and therefore resulting in incorrect values.

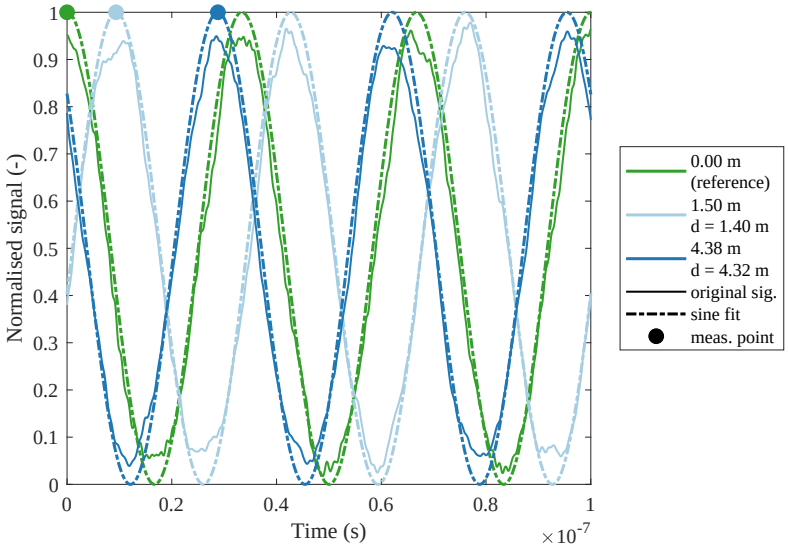

Figure A.3: Delay measurements for amplitude modulation with calibrated reference. 30 MHz amplitude modulated signal is approximated to sine curve. Both original data and sine are normalised. Two distances from the reference point are shown. In the legend tape measured distance is shown and LiDAR calculated distance is bellow. This graph also suggests why distance measurement at this frequency is not very precise as the signal is distorted and down-sampled and therefore the sine fit is not exact.

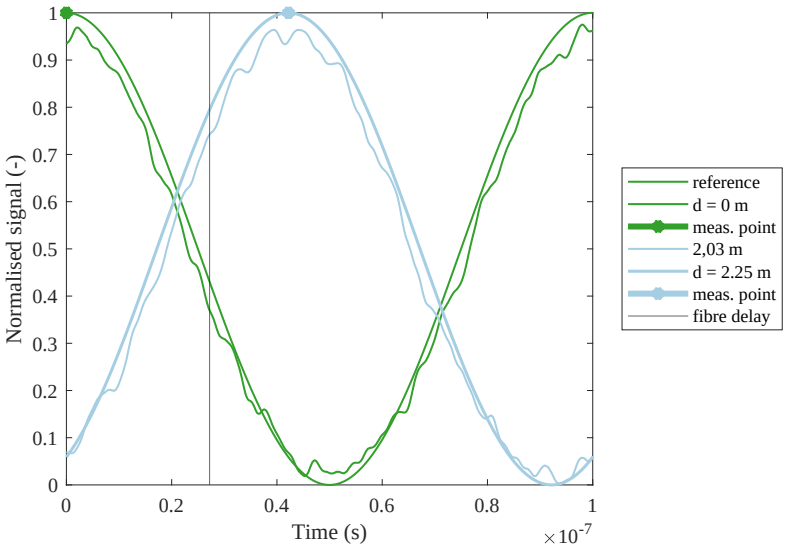

Figure A.4: Delay measurements for amplitude modulation with reference photodiode placed after a beam splitter. 10 MHz amplitude modulated signal is approximated to sine curve. Both original data and sine are normalised. One distance from the reference point are shown. In the legend tape measured distance is shown and LiDAR calculated distance is bellow. This measurement is not as precise because it is not calibrated and involves subtracting of the path trough the optical fibre.